ENGINEERING PRINCIPLES OF AGRICULTURAL MACHINES

Ajit K. Srivastava
Carroll E. Goering
Roger P. Rohrbach

ASAE Textbook Number 6
Published by the
American Society of Agricultural Engineers

Pamela DeVore-Hansen, Editor
Books & Journals
June 1993

8

Hay and Forage Harvesting

Introduction

Domesticated animals have been used as power sources and/or as food during the entire recorded history of agriculture. Through grazing, animals are able to make use of grasses, legumes, and other forage crops that people cannot consume directly. The climate permits year around grazing in some parts of the world. Because grazing is selective and management intensive, however, forages are generally machine harvested and stored for later feeding. The two most common methods of preserving forage crops are as direct cut or field wilting. Ensilage involves cutting the forage at 70 to 80% moisture, allowing it to field dry to 50 to 65% moisture, chopping it into short lengths to obtain adequate packing, and preserving it by fermentation in an airtight chamber. For hay harvest, the forage must be cut and allowed to dry to a moisture content of 15 to 23% before it can be stored. Hay has low bulk density and does not flow readily; silage has the same limitations, plus it will spoil if it is not fed soon after removal from storage. Thus, both hay

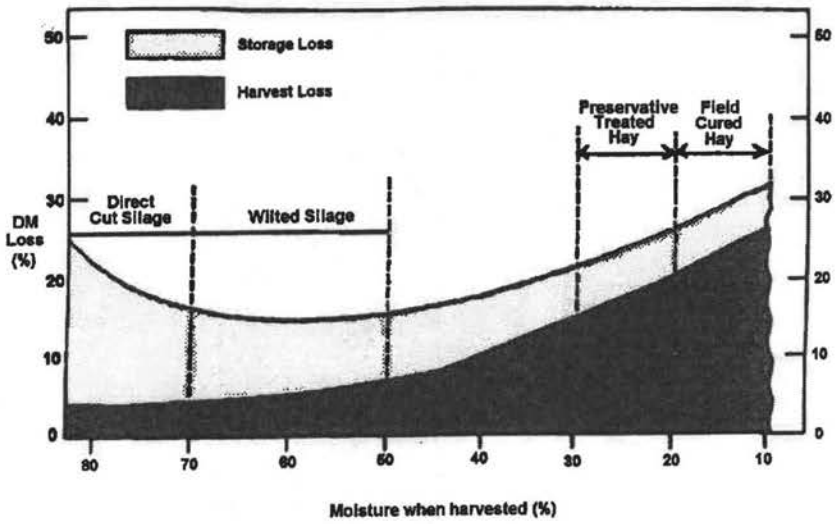

Figure 8.1–Effect of moisture on dry matter losses from forage during harvest and storage.

and silage are often fed close to the point of production. There are, however, commercial hay farms that produce high-quality hay, bale it and ship it considerable distances to customers.

Forages are unique because they are harvested at the peak of moisture content. Because of the large volume of water that must be removed and the limited crop value, it is generally not feasible to dry forages by artificial means. Losses and storage properties are highly dependent on crop moisture (fig. 8.1).

8.1 Methods and Equipment

Figure 8.2 illustrates two common methods for harvesting forage. For harvesting as silage, the standing or wilted crop is cut, field cured and then chopped into short lengths by a forage harvester (fig. 8.3). The same machine conveys the chopped forage into a wagon or truck for transport to the silo. There, the chopped forage is dumped directly

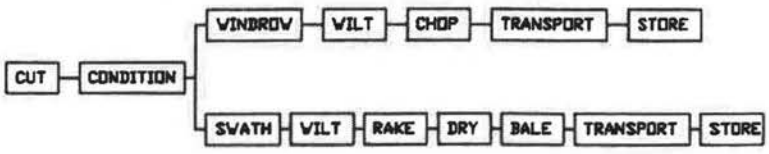

Figure 8.2–Block diagrams of two common forage harvesting methods.

Figure 8.3–A forage harvester (Courtesy of Deere and Co.).

into a bunker silo or, with a tower silo, a forage blower is used to convey the chopped forage into the silo (fig. 8.4). Most grass and legume forage is allowed to partially dry by wilting before chopping; silage stored too wet produces effluents and causes poor fermentation, while that too dry packs poorly and spoils. Therefore, once the crop has reached the proper moisture content (fig. 8.1), the forage harvester and its complementary equipment must provide for a rapid harvest. Direct-cut corn (maize) can be ensiled without drying, since the fermentation process prevents spoilage.

Forages are field dried in either a swath or a windrow. A swath approaches the width of the cut strip, generally leaving enough stubble uncovered to permit wheel traffic during subsequent operations. Swaths dry more rapidly due to greater area exposed to solar radiation, but they must be raked into a windrow for harvesting. A windrow is a narrow strip of forage that dries at a slower rate but does not require further manipulation before harvest. Forages to be made into dry hay are usually placed in a swath while those to be made into silage are placed directly into a windrow to control the drying rate.

Leaves dry faster than stems with legume and grass-type forages. The leaves, especially in legumes, are higher in nutritional value than the stems. Brittle, dry leaves may be lost during raking and harvesting. To reduce such losses, the forage will be conditioned

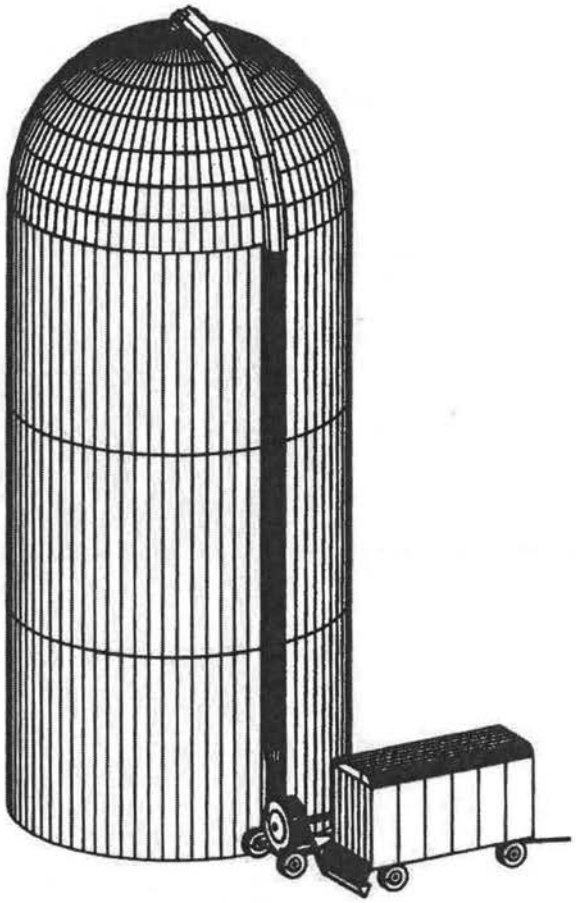

Figure 8.4–Conveying forage into a silo.

so that the stems dry at a rate approaching that of the leaves. Conditioning is a physical process of crushing, cracking or abrading the stems, or a chemical process which dissolves the waxy cutin layer of the stems. Either process improves the stem-drying rate by reducing the natural resistance to moisture removal from the stems.

Grass and legume forages are usually cut with a machine which combines the cutting and the conditioning process (fig. 8.5). The mower-conditioner can place the forage into either a wide swath or a narrow windrow. A windrower can be used to harvest either forages or small grains, but can only place the material into a narrow windrow.

After the forage dries to 23% moisture or less, it is usually compressed to some degree before being transported to storage.

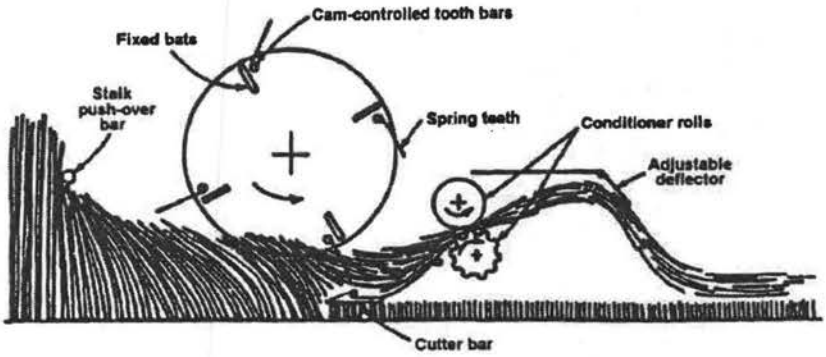

Figure 8.5–Schematic, cross-sectional view of a mower-conditioner. Side deflectors that can be used to form a windrow are not shown.

Baling the hay into rectangular bales of 25 to 40 kg mass (fig. 8.6) provides hay packages that are convenient to store and can be lifted by a single person or by machine. Because they do not resist water penetration very well, rectangular bales are usually transported and stored under a roof soon after baling. In another alternative, the hay is rolled into large round bales of 100 to 500 kg mass (fig. 8.7) which are more resistant to water penetration, especially if plastic wrapped, and are sometimes stored outdoors, although storage losses will be higher. The large round bales are too heavy to be handled by hand, so specialized powered equipment has been developed for handling and transporting such bales. Another approach is to package the hay into

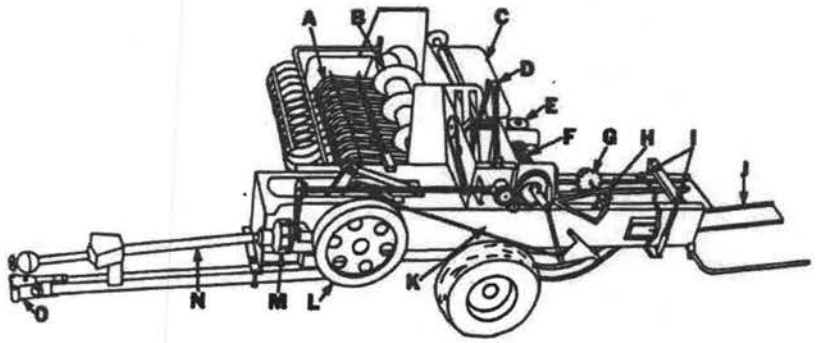

Figure 8.6–A baler that compresses hay into rectangular bales: A = pickup, B = feed auger, C = twine box, D = feed fork, E = hydraulic pump for density control, F = knotter, G = metering wheel, H = metering arm, I = density control rams, J = bale chute, K = bale chamber, L = flywheel, M = slip clutch, N = pto drive, O = hitch (Courtesy of Prairie Agricultural Machinery Institute, Canada).

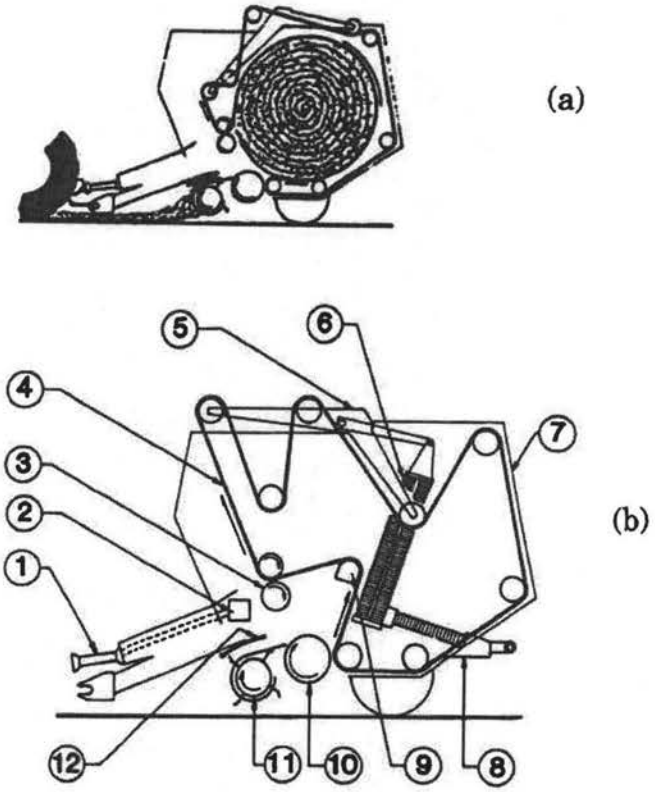

Figure 8.7–Baler for large round bales showing (a) operation and (b) construction details: 1 = drive shaft, 2 = gear box, 3 = stripper roll, 4 = chamber belt, 5 = tensioning arms, 6 = tensioning springs, 7 = tailgate, 8 = bale ejector, 9 = core-forming cam idler, 10 = floor roll, 11 = pickup, 12 = windguard (Courtesy of Prairie Agricultural Machinery Institute, Canada).

large rectangular bales which are similar in weight and density to large round bales. The large rectangular bales will not shed water and thus cannot be stored outdoors, but are better suited to shipping by truck than large round bales.

In addition to those mentioned above, numerous other methods have been developed for harvesting hay. These include pelleting, stacking the hay into stacks in the field, compressing the hay into large loaves, and other methods. Specialized equipment has been developed to support each of these methods. Space does not permit an engineering analysis of all of this diverse equipment, so such analyses will be confined to mowing, conditioning, raking, forage chopping, and baling.

8.2 Functional Processes

8.2.1 Cutting Mechanics and Plant Structure

Mowing and forage chopping involve the cutting of plant materials and cutting will be subjected to engineering analyses in this chapter. Those same analyses have wider application. For example, sickle bar mowers are used for cutting hay and forage, but similar sickle bars are included on the combines that harvest wheat, soybeans and other crops. Thus theory learned in this chapter will be useful in understanding Chapter 9 and perhaps in analyzing machines not covered in this textbook.

Cutting geometry. In a number of agricultural machines, a knife is used to sever plant material. Often severing is accomplished by shearing the material between a moving knife and a stationary countershear. In designing equipment to accomplish the severing, the objectives are to maintain the quality of the harvested product while minimizing the force and energy needed to accomplish the task. The characteristics of both the cutting device and the plant must be considered in pursuing these objectives.

Figure 8.8 illustrates the geometry associated with a mower in which a knife (sickle section) moves with reciprocating motion. The plant material is sheared as the sickle section reaches and passes over the countershear (ledger plate) on the right. At the instant illustrated in figure 8.8, the knife is just leaving the left end of its stroke and moving toward the ledger plate. Guards direct the plant material between the knife and ledger plate and also shield the blunt ends of the sickle sections while they reverse directions at the ends of their stroke.

Typically, in cutting theory, the x-axis of the coordinate system is in the direction of knife movement relative to the plant material. In figure 8.8, the knife has a velocity component, v_{km}, relative to the mower and a component, v_f, due to the forward speed of the mower. The vector sum of these two components gives the knife velocity, v_{kg}, relative to the ground. Since the plants to be cut are attached to the ground, v_{kg} is also the knife velocity relative to the uncut plants. Therefore, the x-axis is in the direction of v_{kg}, the y-axis is in the plane of the paper but perpendicular to x, and the z-axis is perpendicular to the plane of the paper and points upward. Note that the orientation of the coordinate system in figure 8.8 is for only one instant in time, since the magnitude of v_{km} varies during the cutting stroke and thus the coordinate system rotates about the z-axis as the direction of v_{kg} varies.

It is common knowledge that a sharp knife aids cutting. It is important, however, to distinguish between sharpness and fineness. A fine knife has a small bevel angle, ϕ_{bk}, while a blunt knife has a

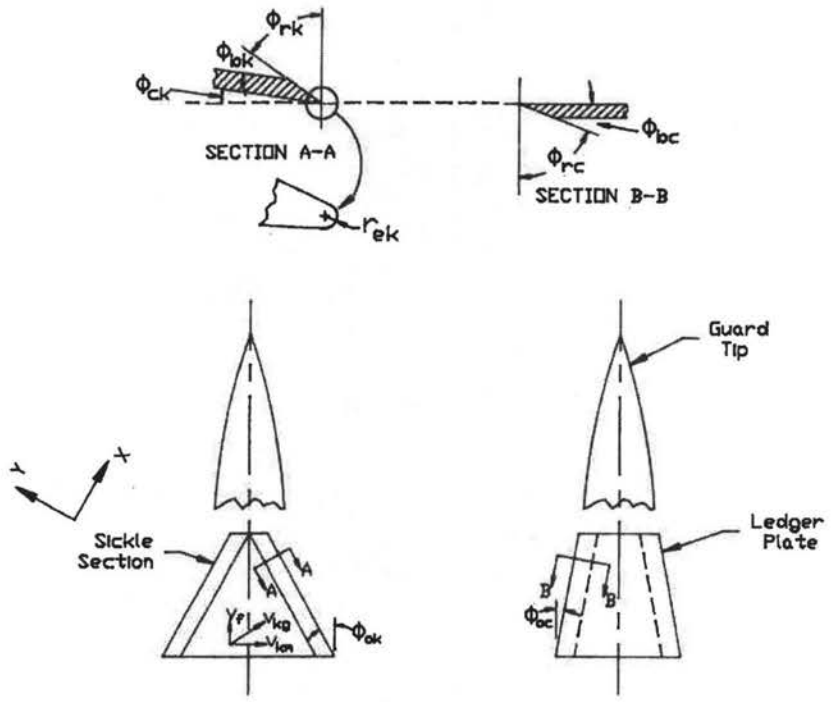

Figure 8.8–Illustration of geometry of a knife and countershear.

large bevel angle. Sharpness is defined by the edge radius, r_{ek}, of the knife, i.e., a sharp knife has a small radius while a dull knife has a larger radius. Initial penetration of the knife into the plant material is aided if the knife rake angle, ϕ_{rk}, is large. The knife clearance angle, ϕ_{ck}, is the angle formed between the bottom edge of the knife and the x-y plane. In general, the following relationship holds between the rake, bevel and clearance angles:

$$\phi_{rk} + \phi_{bk} + \phi_{ck} = 90° \tag{8.1}$$

The chip angle on the knife, ϕ_{chk}, is defined as follows:

$$\phi_{chk} = \phi_{bk} + \phi_{ck} \tag{8.2}$$

The oblique angle of the knife, ϕ_{ok}, is the angle between the y-axis and the cutting edge. The ϕ_{ok} illustrated in figure 8.8 is for the special case where $V_f=0$. A straight cut is one in which $\phi_{ok}=0$.

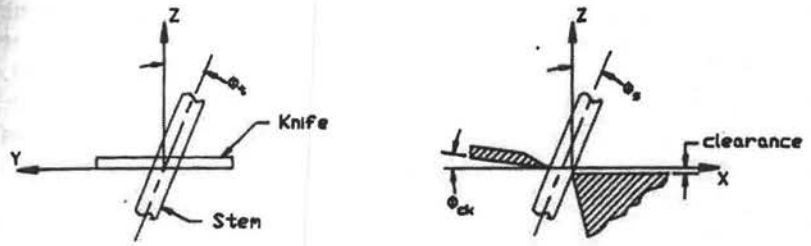

Figure 8.9–Illustrations of stem misalignment.

Conversely, an oblique cut is one in which ϕ_{ok} is not equal to zero. Oblique cutting reduces the peak cutting force because the plant material is sheared progressively rather than all at once as in a straight cut.

The bevel, rake, clearance, and oblique angles all have their counterparts on the countershear, as shown in figure 8.8. For each of these angles, the subscript k indicates that it relates to the knife, while a subscript c indicates the corresponding angle on the countershear. The clip angle, ϕ_{cl}, is the angle formed between the knife and countershear, i.e.:

$$\phi_{cl} = \phi_{ok} + \phi_{oc} \tag{8.3}$$

Frequently, plant stems are not parallel to the z-axis. Figure 8.9 illustrates the tilt angle, ϕ_t, and the slant angle, ϕ_s, which are used to define the orientation of such stems. The tilt angle is the angle between the stem axis and the z axis projected into the y-z plane, while the slant angle is the angle between the stem axis and the z axis projected into the x-z plane. Figure 8.9 also illustrates a positive clearance angle on the knife and the clearance that may be present between the knife and the countershear.

When ϕ_{ok} is not zero and the plant material is not yet in contact with the countershear, the possibility exists that the plant material may slide along the edge of the knife before or while being cut. The sliding is expected if the oblique angle is greater than the following maximum angle:

$$\phi_{okmax} = \arctan\ f_{ek} \tag{8.4}$$

where f_{ek} = knife edge friction coefficient. The edge friction coefficient is the lateral force (parallel to the knife edge) imposed by the plant on the knife edge divided by the normal force imposed by the plant. When the plant is in contact with both the knife and countershear, sliding is expected if the clip angle is greater than the following maximum:

$$\phi_{clmax} = \arctan \frac{f_{ek} + f_{ec}}{1 - f_{ek} f_{ec}} \tag{8.5}$$

where

ϕ_{clmax} = maximum value of ϕ_{cl} that will prevent sliding
f_{ek} = friction coefficient for knife edge
f_{ec} = friction coefficient for countershear edge

Since the forward motion of the mower helps to push the plants toward the rear of the knife sections, sliding is most likely to occur when V_f is small. To increase friction and thus prevent sliding, serrations may be cut into the edge of the knife and/or countershear. For example, values of f_{ek}=0.306 for a smooth knife edge and f_{ec}=0.364 for a serrated ledger plate were observed during cutting of flax straw.

Plant structure. Cutting is a process which causes mechanical failure of plant stems and/or leaves and thus the structure and strength of plant materials are of interest. The engineering properties of plant parts are not as well understood as those of more common engineering materials such as steel, but some engineering studies of plant materials have been made. Living plants consist of solid materials which surround air and liquid-filled cavities. Fiber cells, with diameters of 10 to 50 μm and lengths exceeding 30 mm, provide the main strength of the plant material. Fiber cell walls include three basic layers, the middle lamella, the primary wall, and the secondary wall, with combined thicknesses on the order of 500 nm. The secondary wall lies inside the primary wall and provides the strength and flexibility of the structure. Cellulose chains, the main ingredient of the secondary wall, are bound together in parallel microfibrils of considerable length and with cross-sectional dimension of 2.5 to 20 nm (fig. 8.10). The microfibrils are oriented in spirals, and the angle of the spiral relative to the cell axis determines the elasticity of the cell wall. The cell wall density is approximately 1.45 g/mm^3, but makes up only a small proportion of the cross-section. Some cell walls have strength approaching that of steel, but the numerous cavities greatly reduce the average strength of the plant cross-section.

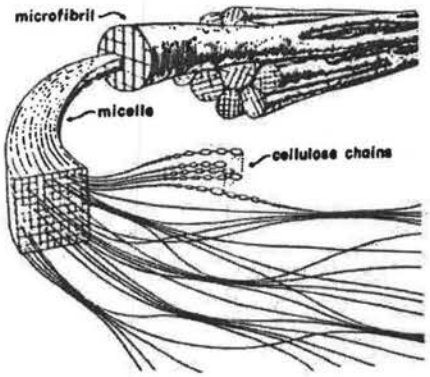

Figure 8.10–Arrangement and structure of microfibrils (Reprinted from *Mechanics of Cutting Plant Materials*, Persson, 1987).

Plant stems and leaves consist of large numbers of similar cells. Structurally, the stems can be viewed as materials with fibers of high tensile strength oriented in a common direction and bound together by material of much lower strength. The softer cells make use of their turgor (liquid pressure) to connect and support the fibers. Grasses, including small grains and corn (maize), and legumes are the materials most commonly involved in agricultural cutting processes, so their structure and strength are of special interest. Many grass stems have hollow internode sections joined by solid nodes (fig. 8.11). The internode sections are much weaker than the nodes and thus determine the stem strength. The corn stalk has internode sections which are not hollow but have a more uniform cross-section. Figure 8.12 shows simplified models that were drawn to represent the actual cross-section of a hollow stem for analyzing stem strength in bending. The strength is determined by the amount of structural fibers and their locations in the plant, rather than by the outside dimensions.

Secondary cell walls in their natural position have ultimate tensile strengths ranging up to 1100 N/mm^2, a modulus of elasticity in the range from 10,000 to 100,000 N/mm^2, and ultimate strain of 0.5 to 5%. Those subject to compression in the growing plant have lower tensile strength but greater elasticity. Other cell walls have much lower strength; for example, tensile strength of the epidermis (skin) ranges from 2 to 14 N/mm^2. Ultimate tensile strength of the solids portion of timothy or alfalfa stems ranges from 90 to 470 N/mm^2; when the entire cross-section of the alfalfa stem is used, the ultimate strength is only 8 to 35 N/mm^2.

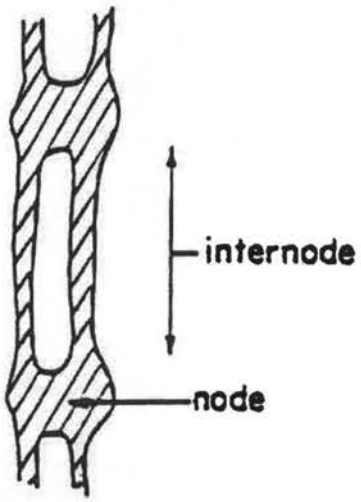

Figure 8.11–Longitudinal section through a stem, showing nodes and internodes (Reprinted from *Mechanics of Cutting Plant Materials*, Persson, 1987).

The bending strength of a plant stem may be important during cutting. For example, some devices cut a plant in the absence of a countershear; the plant stem below the cutting plane is loaded as a cantilever beam. In other situations, the stem may be loaded as a simply-supported beam. In either case, the direction of loading is radial (perpendicular to the longitudinal axis of the plant stem). The radial load that would cause failure in bending can be calculated using the following equation:

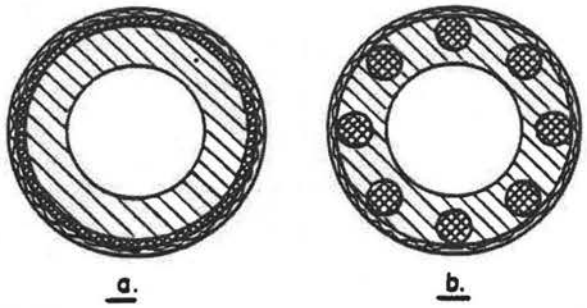

Figure 8.12–Mechanical equivalents stem cross-sections, showing the main structural components arranged as (a) a concentric cylinder, and (b) eight reinforcement rods. Drawn to approximate scale with regard to area and moments of inertia in bending (Reprinted from *Mechanics of Cutting Plant Materials*, Persson, 1987).

$$F_{bu} = \frac{I}{c}\frac{S_u}{L} \tag{8.6}$$

where

F_{bu} = ultimate load at bending failure (N)
I = moment of inertia of the cross-section (mm^4)
c = radius from neutral axis of stem to most distant load-carrying fiber (mm) or, alternately
I/c = section modulus (mm^3)
S_u = ultimate stress of plant fibers (N/mm^2)
L = distance from concentrated load to point of support (mm)

The deflection of the stem is given by equation 8.7, i.e.:

$$\delta_r = \frac{F_r L^3}{C_b E I} \tag{8.7}$$

where

δ_r = radial deflection (mm)
F_r = radial concentrated load (N)
E = modulus of elasticity of stem fibers (N/mm^2)
C_b = constant (3 for cantilevered beams, 48 for simply-supported beams)

The moment of inertia of a homogeneous solid, circular section is:

$$I = \frac{\pi d^4}{64} \tag{8.8}$$

where d = diameter of the section (mm). For a hollow, thin-walled section, the moment of inertia is:

$$I = \frac{3 \pi d^3 t}{32} \tag{8.9}$$

where t = wall thickness (mm). From comparing equations 8.8 and 8.9, we note that the moment of inertia of a natural stem should be proportional to the section diameter raised to an exponent between 3 and 4. Similarly, assuming that the neutral axis is centered in the stem, the section modulus should be proportional to

Figure 8.13–Cross-section of a stem (a) before and (b) after compression (Reprinted from *Mechanics of Cutting Plant Materials*, Persson, 1987).

the diameter raised to an exponent between 2 and 3. The appropriate section diameter is determined by the location of the cell-wall fibers rather than the outside diameter (see fig. 8.12) and thus, if the outside diameter is used, the bending strength will be somewhat over estimated. If loading crushes a stem prior to cutting (see fig. 8.13), the circular cross-section no longer exists; the moment of inertia and section modulus must then be calculated for the new geometry of the cross-section.

The size and bending strength of plant stems increases with plant maturity (Persson, 1987). For example, the stem dry mass of timothy increased from 0.6 to 1.4 mg/mm of length as the plant matured; the corresponding stiffness (EI) increased from 1260 to 3900 $N \cdot mm^2$. For red fescue (which has a much finer stem) at 67% moisture content, the corresponding figures were stem dry mass increasing from 0.017 to 0.083 mg/mm as the plant matured, while the stem stiffness increased from 0.53 to 5.7 $N \cdot mm^2$. The stiffness of timothy stems was found to vary with diameter raised to an exponent between 2.66 and 2.99. For cotton stalks ranging in diameter from 7 to 16 mm, the stiffness varied with diameter to the 3.0 power. The modulus of elasticity of cotton stalks ranged from 600 to 3500 N/mm^2. Moisture content affects the strength of plants, since the turgor pressure in the cells affects stem rigidity and strength. Since plants must resist wind loading, strength also varies with height on the plant, i.e., most plants are larger and stronger near the ground than at the top. Near the base of rice straw at 62% moisture

content, for example, the stems were 3.5 to 4 times heavier per unit length than near the top. Calculation of plant strength and deflection is illustrated in example problem 8.1.

Example Problem 8.1

A living alfalfa stem of 2.5 mm diameter is loaded horizontally at a distance 30 mm above the soil surface, that is, it is loaded as a cantilever beam. Based on the entire stem cross-section, the modulus of elasticity is 1500 N/mm^2 and the ultimate tensile strength is 35 N/mm^2. (a) Calculate the horizontal force that would cause bending failure. (b) Calculate the horizontal deflection of the stem at point of failure.

Solution. (a) Before using equation 8.6 to calculate the ultimate load, it is necessary to calculate the section modulus, I/c, of the stem. The value of c is half the stem diameter, or 1.25 mm. From equation 8.8, the moment of inertia is:

$$\pi \cdot 2.5^4/64 = 1.92 \text{ mm}^4$$

The $I/c = 1.92/1.25 = 1.53 \text{ mm}^3$. Then, from equation 8.6, the ultimate bending load is:

$$F_u = 1.53 \cdot 35/30 = 1.79 \text{ N}$$

(b) Now, equation 8.7 can be used to calculate the stem deflection:

$$\delta_r = 1.79 \cdot 30^3/(3 \cdot 1500 \cdot 1.92) = 5.6 \text{ mm}$$

For this example, the stem would deflect 5.6 mm before the stem fibers failed in bending.

Mechanics of cutting. Several different modes of tissue failure can occur during cutting, depending upon the knife characteristics. Initial penetration of the knife results in localized plastic deformation (flow) of the plant material. In moist stems and with high knife speeds, turgor pressure in the stems limits initial compression of the plant. With further knife movement, considerable stem buckling and compression occurs (see fig. 8.13); depending on knife sharpness and speed, the compression can advance well ahead of and to the sides of the knife edge. The precompression before failure results in a gradual buildup of force on the knife and the energy for precompression can consume 40 to 60% of the total cutting energy. As the fibers are deflected ahead of the knife edge, the shear strength of the material is mobilized to produce fiber tensile stresses. These stresses become sufficiently large to cause the fibers to fail in tension, whereupon loading is transferred to fibers further ahead of

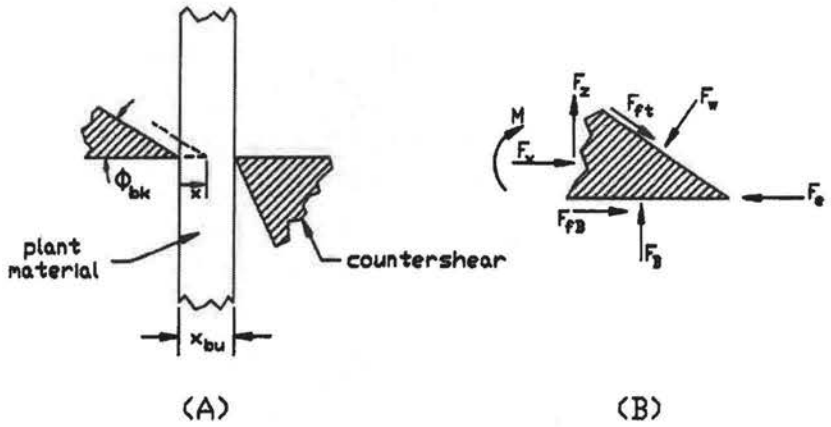

Figure 8.14–Illustration of knife forces during cutting.

the knife edge. For common crop materials, cutting occurs when the pressure exerted ahead of the knife edge exceeds 9 to 30 N/mm^2.

Figure 8.14a illustrates a knife and countershear cutting a bed of plant material. Forces on the knife are illustrated in figure 8.14b. The force, F_x, in the direction of knife motion is the sum of the knife edge force plus x-components of forces imposed on the top and bottom surfaces of the knife as it compresses and penetrates the plant material. By assuming that only the material directly ahead of the knife is compressed and by use of the bulk modulus for the plant material, the following equation for knife force was derived:

$$\frac{F_x}{w} = \frac{F_{ek}}{w} + \frac{B_f x^{\lambda}}{2 X_{bu}} \cdot (\tan\phi_{bk} + 2 \cdot f) \qquad (8.10)$$

where

F_x = knife driving force in x direction (N)
F_{ek} = force imposed by plant on the knife edge (N)
w = width of knife (mm)
x = knife displacement after initial contact (mm)
λ = exponent
B_f = bulk modulus of forage (N/mm^2)
X_{bu} = uncompressed depth of material between knife and countershear (mm)
f = coefficient of friction of forage on knife
ϕ_{bk} = bevel angle of knife edge

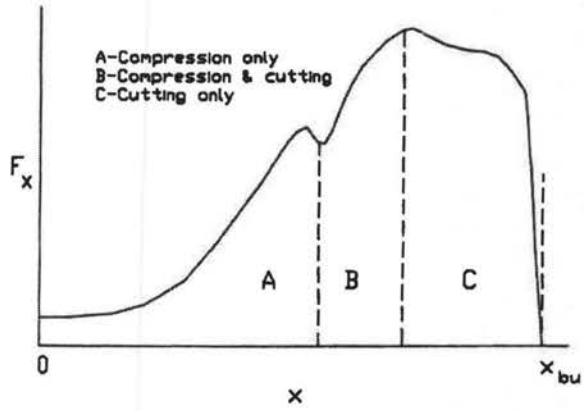

Figure 8.15–Knife force-displacement curve for a straight cut against a countersheet.

Theoretically, $\lambda=2$ in equation 8.10. However, a smaller exponent gives a better fit to some experimental cutting data. In an experiment in which a thin (8.9 mm) bed of timothy at 20% moisture was cut at a very low (0.42 mm/s) knife speed, equation 8.10 fits the data when $\lambda=1.46$ and $B_f=10$ N/mm^2. The knife edge force is calculated as the product of the projected frontal area of the knife edge times the pressure imposed on that edge by the forage. The approximate frontal area can be calculated from the following equation:

$$A_{ek} = r_{ek}\left(1 + \cos\left(\phi_{bk} + \phi_{ck}\right)\right) \tag{8.11}$$

where

A_{ek} = frontal area of knife edge per mm of width (mm^2)
r_{ek} = radius of knife edge (mm)

Figure 8.15 shows the typical shape of the force-displacement curve when plant material is cut by a knife and countershear. In Section A, only compression occurs as the knife edge force is not yet high enough to cause cutting. After initial stem failure, some compression continues in Section B along with cutting. In section C, the material is fully compressed; cutting continues and then the force drops rapidly as the knife edge crosses the edge of the countershear. With suitable choice of parameters, the force in sections A and B could be calculated using equation 8.10. Section C does not involve compression so equation 8.10 does not fit that section. The diagram

in figure 8.15 is for a straight cut, i.e., with $\phi_{cl}=0$. For an oblique cut, the peak cutting force would be reduced and the duration of cut would be extended compared to figure 8.15.

Figure 8.15 is useful in calculating the power requirement for cutting with a knife and countershear. The energy per cut is equal to the area under the cutting force curve; multiplying by the cutting frequency gives the power. The following equation can be used to compute the power requirement for cutting:

$$P_{cut} = \frac{C_F F_{xmax} X_{bu} f_{cut}}{60{,}000} \tag{8.12}$$

where

P_{cut} = power for cutting (kW)
F_{xmax} = maximum cutting force (kN)
X_{bu} = depth of material at initial contact with knife (mm) (see fig. 8.15)
f_{cut} = cutting frequency (cuts/min)
C_F = ratio of average to peak cutting force

C_F is always between 0 and 1 and, for a typical force-displacement curve as illustrated in figure 8.15, it is approximately equal to 0.64.

The cutting force, F_x, must be supported. If a countershear is present and clearance is small, the support force can be provided entirely by the countershear. When no countershear is present, the support force must be provided entirely by the plant itself through the bending strength of the stump below the cut and the inertia of the plant above the cut. The resulting cut is called, alternatively, an impact cut, an inertia cut or a free cut. As clearance with a countershear increases, the plant strength and inertia come increasingly into play; thus, impact cutting is similar to countershear cutting with very large clearance. Figure 8.16 illustrates the forces and moments on the plant during impact cutting. The soil and the plant root system provide a force, F_B and a moment, M_r, which tend to keep the stump upright. Acceleration of the stump is considered to be negligible. Force F_B represents the combined effects of the root system and stalk strength in providing bending resistance at the height of the cut. The center of gravity of the cut portion of the plant is at a height, z_{cg}, above the cut. The impact shown in figure 8.16 tends to accelerate the cut plant to the right and counterclockwise; consequently, an inertia force and inertia moment appear on the plant at the center of gravity. The following equation results from summing moments about the center of gravity of the cut plant:

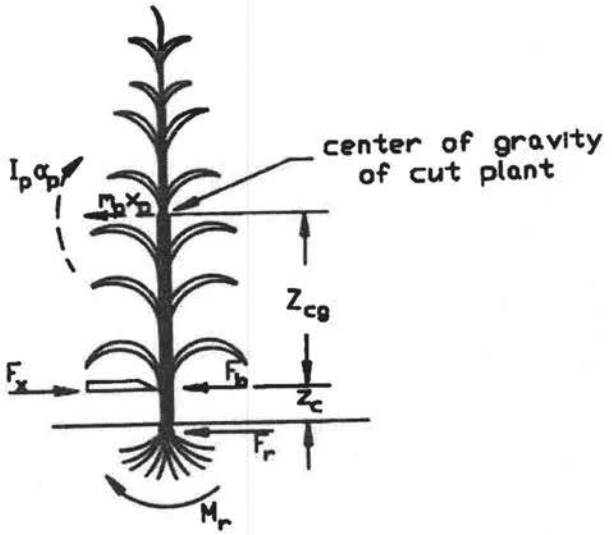

Figure 8.16–Forces and moments in impact cutting.

$$I_p \alpha_p = (F_x - F_b) z_{cg} \tag{8.13}$$

where

α_p = angular acceleration of plant (rad/s^2)
F_x = cutting force (N)
F_b = bending resistance of stump (N)
z_{cg} = height of center of gravity of cut plant (m) (see fig. 8.16)
I_p = centroidal moment of inertia of plant (kg·m^2 = $m_p \cdot r_g^2$)
m_p = mass of cut portion of plant (kg)
r_g = radius of gyration of cut portion of plant (m)

An analysis of the kinematics (motions) of the plant gives the following equation for angular acceleration:

$$\alpha_p = \frac{a_c - a_{cg}}{z_{cg}} \tag{8.14}$$

where

a_c = acceleration of plant at plane of cut (m/s^2)
a_{cg} = acceleration of plant center of gravity (m/s^2)

By assuming that the plant acquires knife velocity at the plane of cut, the following equation was derived:

$$a_c = \frac{1000\, v_k^2}{d_s} \tag{8.15}$$

where

v_k = knife velocity (m/s)
d_s = stalk diameter at plane of cut (mm)

Equations 8.13 through 8.15 can be combined to give the following equation for minimum knife velocity for impact cutting:

$$v_k = \sqrt{d_s \frac{(F_x - F_b)}{1000 * m_p}\left(1 + \frac{z_{cg}^2}{r_g^2}\right)} \tag{8.16}$$

When values for r_g and z_{cg} are not readily available, a simpler approximate equation can be obtained by assuming that $r_g = z_{cg}$. The simpler equation illustrates the key variables involved in impact cutting. If the stump bending resistance, F_b, is large enough to support the entire cutting force, F_x, the minimum required knife velocity is zero and cutting is equivalent to cutting with a countershear. Lowering the height of cut to increase F_b and reducing F_x by maintaining a sharp knife will both reduce the minimum required knife velocity. Tests of impact cutting of timothy, for example, have shown that cutting could be accomplished at knife velocities as low as 25 m/s but velocities of 45 m/s were required for reliable cutting of all stems. To assure reliable cutting over a wide range of knife sharpness and stem stiffness, minimum knife velocities of 50 to 75 m/s are generally recommended. Example Problem 8.2 illustrates the calculation of minimum knife velocity for impact cutting.

Example Problem 8.2

Impact cutting is to be used to cut the alfalfa stem of example problem 8.1 at a height 30 mm above the ground. The mass of the plant above the cut is 0.01 kg. Assume that cutting occurs when the pressure ahead of the knife edge reaches 25 N/mm^2. The knife has a bevel angle of 20°, zero clearance angle, and an edge radius of 0.3 mm. Calculate (a) the force imposed by the knife edge to achieve cutting, (b) the minimum knife speed required for impact cutting.

Solution. (a) The frontal area of the knife edge can be calculated using equation 8.11:

$$A_{ek} = 0.3 \cdot (1 + \cos(20 + 0)) = 0.582 \text{ mm}^2/\text{mm width}$$

The width of knife is not known but, since only a single stem is being cut, the width will be assumed equal to the stem diameter, 2.5 mm. Then, using the critical pressure of 25 N/mm^2, the force required to initiate cutting will be:

$$F_{ek} = 0.582 \cdot 2.5 \cdot 25 = 36.4 \text{ N}$$

(b) Equation 8.16 is available for calculating the minimum knife velocity for impact cutting. Values for r_g and z_{cg} are not available, but we will assume $r_g = z_{cg}$. No value for F_b is given but we will assume it is equal to the ultimate bending load calculated in Example Problem 8.1, that is, F_b = 1.79 N. Then the minimum velocity is:

$$v_k = [2 \cdot 2.5 \cdot (36.4 - 1.79)/(1000 \cdot 0.01)]^{0.5} = 4.2 \text{ m/s}$$

In this idealized cutting of a single stem, the minimum velocity was low. Typically, to allow for interaction of multiple stems during cutting, velocities of 50 to 75 m/s are recommended.

8.2.2 Cutting and Chopping

Cutting with a countershear. The construction of a typical cutterbar is illustrated in figure 8.17. Terminology for the cutting elements is shown on the detailed cross-sectional view in figure 8.17a. The knife sections and sometimes the ledger plates are replaceable. Knife section edges can be smooth or serrated and either type of sickle can be removed for sharpening. Ledger plate edges are usually serrated on the underside and are not resharpened. The knife clips maintain correct clearance between the knife sections and ledger plates. The wear plates support the rear edges of the knife sections and must be replaced when vertical clearance becomes excessive. In addition to guarding the blunt ends of the knife sections from the oncoming material at each end of the stroke, the guards also help to protect the sickle from being damaged by rocks. Typical guard spacing is 76.2 mm; the sickle stroke can be equal to or up to about 15 mm less than or greater than the guard spacing.

Most forages are harvested with a machine that combines the mowing and conditioning process, hence the name, mower-conditioner. The cutterbar and associated reel (fig. 8.5) are mounted on a separate framework which is connected to the machine by a spring-loaded four-bar linkage. Adjustable shoes are placed at each end of the separate assembly to adjust the cutting height, typically in the range from 25 to 100 mm. The flotation springs are adjustable to provide from 0.3 to 0.4 kN of vertical ground reaction on the shoes.

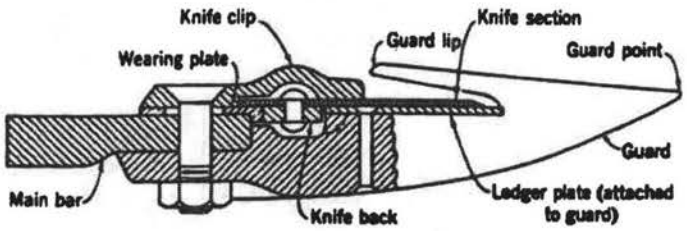

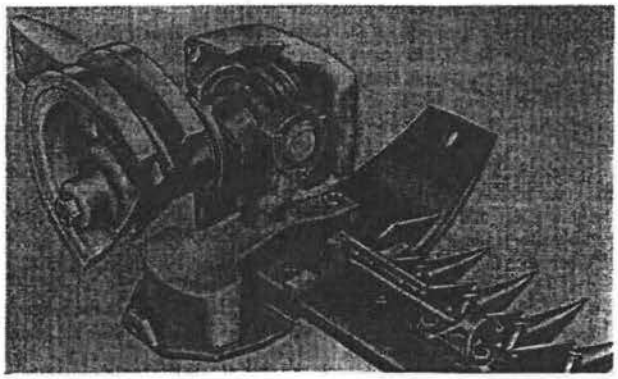

Figure 8.17–A mower cutterbar with drive unit (Reprinted from *Principles of Farm Machinery*, Kepner et al., 1978).

The cutterbar assembly should "float" easily over the ground without bouncing.

The type of pickup reel that is used on a mower-conditioner is also used on other machines, for example, forage harvesters and combines. Figure 8.18 illustrates three different types of mechanisms used in pickup reels. The mechanisms in figures 8.18a and 8.18c keep all of the reel teeth parallel at all times but, because eccentric spider control is simpler and less expensive, it has supplanted the planetary gear control that was previously used. By adjusting the location of the center of the bearing control plate (fig. 8.18a), the pitch of the teeth can be adjusted. Although cam control (fig. 8.18b) is more complex than eccentric spider control, the cam does permit changing the pitch of the teeth on each tooth bar as the bar progresses through its cycle. Thus, the teeth can be given a greater lifting action as they pass near the cutterbar.

The cutterbar should have proper tilt, register, and alignment. Tilt is adjusted by rotating the cutterbar about an axis parallel to the

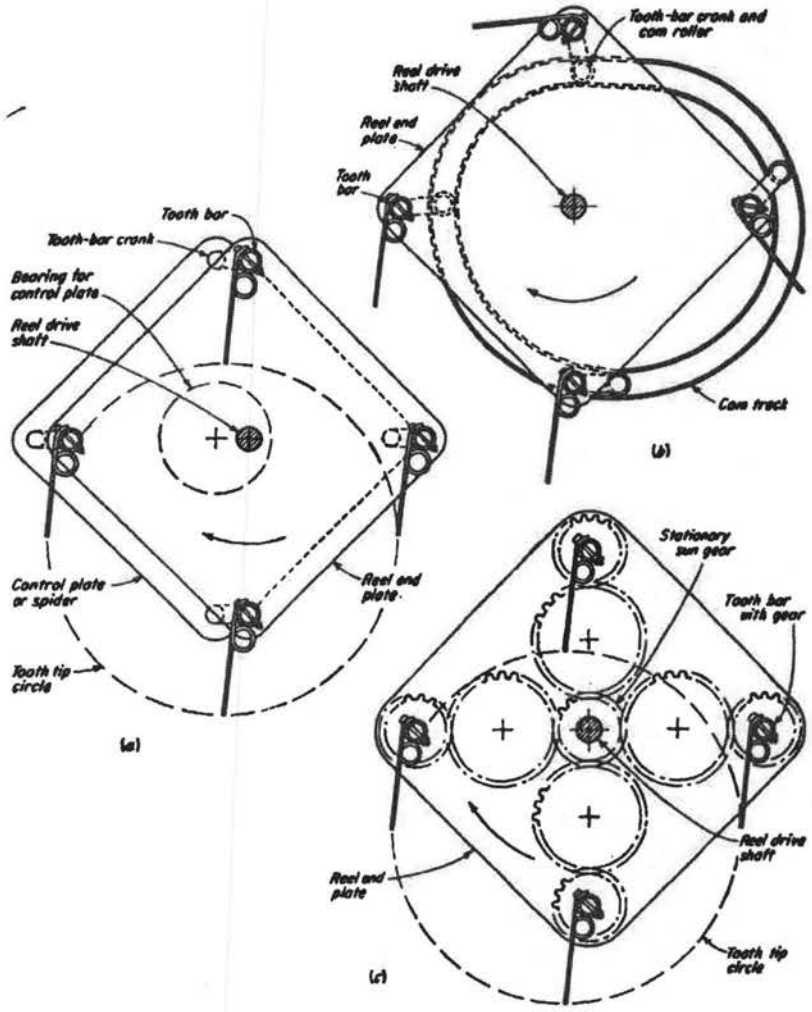

Figure 8.18–Feathering actions used in pickup reels with (a) eccentric spider control, (b) cam control, (c) planetary gear control (Reprinted from Richey et al., 1961).

sickle to raise or lower the guard tips. Proper register is achieved by moving the cutterbar in or out relative to the drive mechanism until the knife stroke is in symmetry with the guard spacing. The cutterbar is in proper alignment when it is perpendicular to the direction of travel while mowing. Alignment is generally not a problem when the cutterbar has horizontal support on both ends. On mowers which have the cutterbar extending outward from one side of the machine, however, the horizontal forces on the cutterbar create a

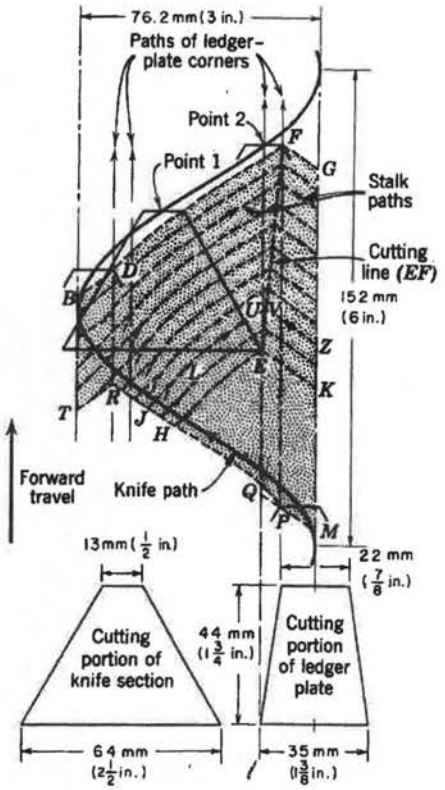

Figure 8.19–Cutting pattern of a conventional sickle bar mower (Reprinted from *Principles of Farm Machinery*, Kepner et al., 1978).

moment and the resulting deflection causes the outer end to lag behind the drive mechanism. To offset the lag, the outer end must lead the drive mechanism by about 20 mm/m of bar length when the mower is not operating. The driveline to the cutterbar should be protected to prevent damage if the sickle becomes jammed. A v-belt in the drive can provide overload protection but, if there is no belt in the drive, a slip clutch or jump clutch should be included in the driveline.

The cutting frequency is a key variable in the operation of a sickle bar mower. A higher cutting frequency aids cutting by increasing v_{km} (see fig. 8.8) and also allows higher travel speeds. Figure 8.19 shows typical dimensions of a sickle section and ledger plate, as well as a typical cutting pattern. Note that plants growing in the area bounded by points KMPQHE on the diagram must be

deflected forward and cut ahead of point E. In figure 8.19, that area is equal to 25% of the total area cut per stroke; such bunching is undesirable because it leads to increased cutting forces and uneven stubble height. To avoid excessive bunching with a conventional mower, the forward travel of the mower should not exceed 150 mm per knife cycle; thus increasing the cutting frequency also increases the maximum allowable travel speed. Since the mowing capacity of the mower varies with the product of the cutterbar width and the forward speed, the maximum mowing capacity is proportional to the cutting frequency. Because the sickle must be reversed in direction at each end of its stroke, vibration imposes an upper limit on cutting frequency. The mower shown in figure 8.17b includes a counterweight which moves opposite in direction to the sickle to reduce the vibrations. Double sickle mowers are available; such mowers have no guards but have two reciprocating sickles moving in opposite directions. Double sickle mowers permit up to 220 mm of forward travel per cycle without excessive bunching and the opposite-moving sickles provide automatic balancing. A major limitation has been that the absence of guards has led to rock damage to the unprotected sickles. Also, some vibration of the cutterbar is desirable because it helps to keep the cut material flowing over the cutterbar.

Two well-known mechanisms are available for converting rotary motion into the reciprocating motion required to drive a sickle, i.e., a slider-crank or a spatial-crank mechanism. The spatial crank is more common because of its compact size and the ease with which it can be integrated into the drive train of a machine.

The spatial-crank oscillator is a mechanism from the Spherical Mechanism Group. Another well-known member of this group is the Cardan universal joint which was described in Chapter three. All of the joint axes in this group of mechanisms intersect at a common point. In the spatial-crank oscillator, the output shaft must be skewed with respect to the input shaft and the angle γ (fig. 8.20) must be smaller than the angle β. In the oscillator shown in figure 8.20, angle β is 90° or 1.57 radians. The following three equations govern the displacement, velocity and acceleration, respectively, of the oscillating shaft equation 8.19 assumes zero input acceleration:

$$\tan(\Gamma) = \tan(\gamma)\sin(\theta) \tag{8.17a}$$

$$\dot{\Gamma} = \frac{\dot{\theta}\tan(\gamma)\cos(\theta)}{1 + \tan^2(\gamma)\sin^2(\theta)} \tag{8.18}$$

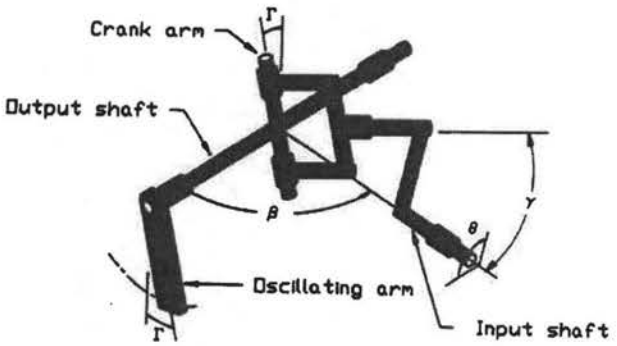

Figure 8.20–Isometric view of a spatial-crank oscillator.

$$\dot{\Gamma} = \frac{-\dot{\theta}\tan(\gamma)\sin(\theta)\left[1+\tan^2(\gamma)\left(1+\cos^2(\theta)\right)\right]}{\left[1+\tan^2(\gamma)\sin^2(\theta)\right]^2} \qquad (8.19)$$

where

Γ = displacement of the oscillating shaft (radians)
θ = rotational displacement of input shaft (radians)
γ = input shaft angle, radians (see fig. 8.20)

The dot notation used in equations 8.18 and 8.19 indicates time derivates of the variables indicated. If $\gamma < 0.33$ radians in equation 8.17, the tangent functions in the equation are approximately equal to the value of the argument in radians and thus the following simplified equation gives the displacement of the oscillating shaft with less than 0.2% error:

$$\Gamma = \gamma \sin(\theta) \qquad (8.17b)$$

An oscillating arm is generally attached to the oscillating shaft to convert the shaft rotational oscillation to the required rectilinear motion required by the sickle. Note, however, that the tip of the oscillating arm travels on an arc rather than in a straight line. The problem is overcome by using a flexible bushing to connect the arm to the knife and by keeping the oscillation angle small and the arm length long within reasonable limits.

Counterbalancing to reduce vibration caused by inertial forces is not generally required because the mass of the machine supporting the cutterbar is so large relative to the mass of the reciprocating knife. However, the vibrations generate stresses, increasing

maintenance problems and the possibility of early fatigue failure of the moving parts. Essentially full dynamic balancing can be obtained by attaching a countermass to the crank arm. For example, if a countermass equal to the sickle mass were attached to the top of the crank arm in figure 8.20 and if the sickle and countermass were vertically equidistant from the output shaft, the horizontal oscillating forces would cancel. There would be a residual oscillating couple due to the vertical separation between the sickle and the countermass.

The approximate velocity of the knife relative to the mower (v_{km}) can be calculated by assuming that the sickle moves with sinusoidal motion. This assumption neglects some higher-order harmonics that may be present depending upon the specific drive used to power the sickle. Assuming sinusoidal motion, the relative sickle speed is given by:

$$v_{km} = \frac{L_s \omega_c}{2000} \cos(\omega_c t) \qquad (8.20)$$

where

v_{km} = velocity of knife relative to mower (m/s)
L_s = stroke length of knife (mm)
ω_c = sickle frequency (rad/s)
t = time measured from center of stroke (s)

Equation 8.20 is useful in estimating the speed of the knife through the cutting zone. Also, as shown in example problem 8.3, equation 8.20 is useful in determining the conditions under which plant material may slide forward on the knife and escape cutting.

Example Problem 8.3.

The oblique angle of the sickle sections is 30° when $v_f = 0$, i.e., when the mower is not moving forward. If the stroke length is 76.2 mm and the cutting frequency is 105 rad/s, what is the minimum v_f at which, during the entire knife stroke, the plant material will move toward the rear of the knife sections rather than moving toward the knife tips to possibly escape cutting?

Solution. Insight can be gained by calculating the conditions under which the oblique angle is zero during cutting since, when the oblique angle is zero, there is no tendency for the material to move along the edge of the knife sections. The oblique angle is zero when the knife movement relative to the ground is perpendicular to the knife edge, i.e., when:

$$v_f / v_{km} = \tan 30°$$

or, by making use of equation 8.20, when:

$$v_f = (L_s\,\omega_c/2000)\cos(\omega_c\,t)\tan(30°)$$

The most critical point is at midstroke (t=0) when the cosine term has its maximum value of 1.0. Then, substituting in the given values of L_s and ω_c, the minimum forward travel speed is:

$$v_f = 76.2 \cdot 105/2000)\cos(0)\tan(30°) = 2.31 \text{ m/s}$$

At v_f = 2.31 m/s, the material will have no y-component of velocity at midstroke but will tend to move toward the rear of the knife sections at all other parts of the stroke. At slower travel speeds, the material will tend to move toward the knife tips at midstroke. Of course, as equation 8.4 indicates, edge friction may be sufficient to keep the material from moving along the edge of the knife sections.

Equation 8.12 can be used to calculate the theoretical power requirement for mowing with a cutterbar mower. However, that equation does not include friction between the knife and cutterbar or other losses. By comparing pto power delivered to a mower while not cutting and while cutting moderately heavy mixed forage, Elfes(1954) found that cutting used only about 30% of the total pto power. Cutting frequency was 942 cycles/min and average total knife force was 1.2 kN/m of bar length. Harbage and Morr (1962) measured an average total knife force of 2.3 kN/m when mowing bluegrass at 1250 cycles/min. ASAE Data D497 suggests a pto power requirement of 1.2 kW/m of bar length for mowing alfalfa. To that must be added the tractive power required to overcome drag on the cutterbar and rolling resistance of the tractor and mower.

Impact cutting, horizontal axis. Impact cutting is used in flail mowers and rotary mowers. As shown in the schematic view of figure 8.21a, the flails in flail mowers rotate about a horizontal, transverse axis. Hinging of the flails provides flexibility for the flails to swing back and minimize damage in rocky fields. Some of the various types of knives used on flail mowers are shown in figure 8.21b. Staggering the flails in the successive rows provides complete coverage of the swath. Early flail mowers suffered excessive losses because short pieces of forage were lost in the stubble. Losses were reduced by designing the shroud to bend the plants forward to permit basal cutting and to provide clearance above the flail to reduce recutting. Bending the plants forward also permits lower knife velocities than calculated by equation 8.16 and the lower knife velocities also reduce recutting. Knife peripheral speeds of 43 m/s or less have been found to be satisfactory. The full-width gage roller

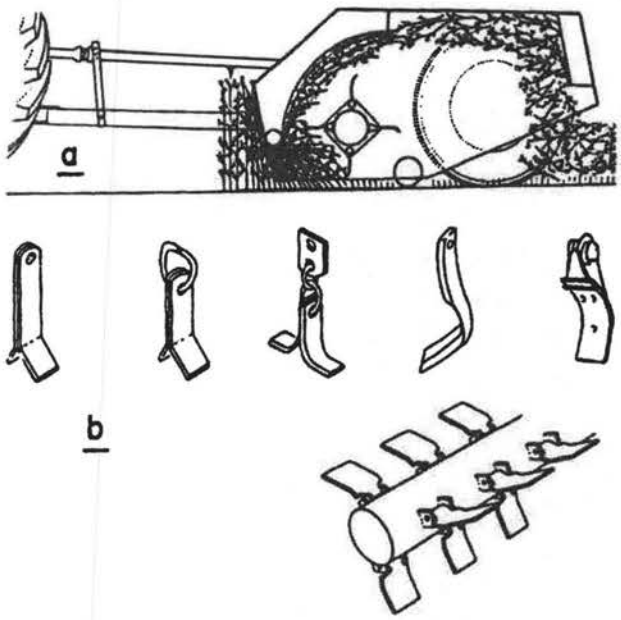

Figure 8.21–A flail mower, showing (a) side view and (b) flail detail (Reprinted from *Mechanics of Cutting Plant Materials*, Persson, 1987).

behind the flail (see fig. 8.21a) provides accurate control of cutting height and prevents scalping of high spots. The hitch of pull-type flail mowers is offset so that the tractor wheels run on cut forage rather than on the standing crop. The lacerating effect of the knives on the stems provides a conditioning effect that helps to increase the drying rate. In upright crops, the flail mower typically recovers 5 to 10% less of the crop than sickle bar mowers. Conversely, the flail mower can recover substantially more of a severely lodged crop.

The tips of the knives on the flail mower trace out cycloidal paths as the mower moves forward over the land. The x,z-coordinates of the path can be calculated using the following equations:

$$\frac{x}{r_f} = \frac{v_f t}{r_f} + \sin \theta_r \tag{8.21}$$

$$\frac{z}{r_f} = 1 - \cos \theta_f \tag{8.22}$$

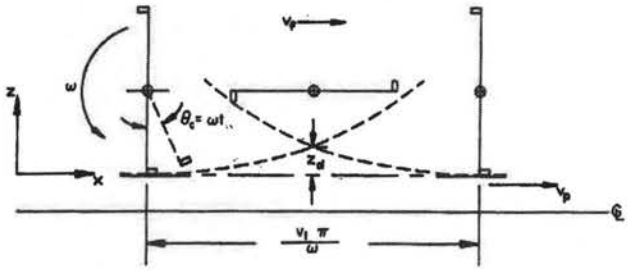

Figure 8.22–Flail mower cutting analysis.

where

x = displacement of the tip in the x-direction (m)
z = corresponding displacement of the tip in the z-direction (m)
r_f = radius to tip of flail (m)
v_f = forward velocity of mower (m/s)
θ_r = angular displacement of rotor, rad (see fig. 8.22
t = time (s)

Theoretically, the stubble height can become uneven if v_f becomes too large in relation to the knife peripheral speed, v_p. The distance, z_d, in figure 8.22 illustrates the uneven stubble height. The following equation can be used to calculate the approximate value of z_d:

$$\frac{z_d}{r_f} = 1 - \cos \frac{\pi}{\lambda_r (1 + C_v)} \tag{8.23}$$

where

z_d = stubble height difference (m)
C_v = velocity ratio = v_p/v_f
λ_r = number of rows of flails on the rotor

Equation 8.23 includes the assumption that the sine of the rotor angle is approximately equal to the value of the angle in radians. For realistic values of C_v, that assumption is valid. Note in figure 8.21b that alternate rows of flails are staggered to assure cutting over the entire swath width. Because of the staggered arrangement and the lateral gaps between the flails, λ_r=2 for the rotor shown in figure 8.21a. Given that a typical v_p for flail mowers is about 43 m/s, C_v is 10 or greater for reasonable travel speeds. Equation 8.23 shows that the flail mower can produce good stubble uniformity under such conditions.

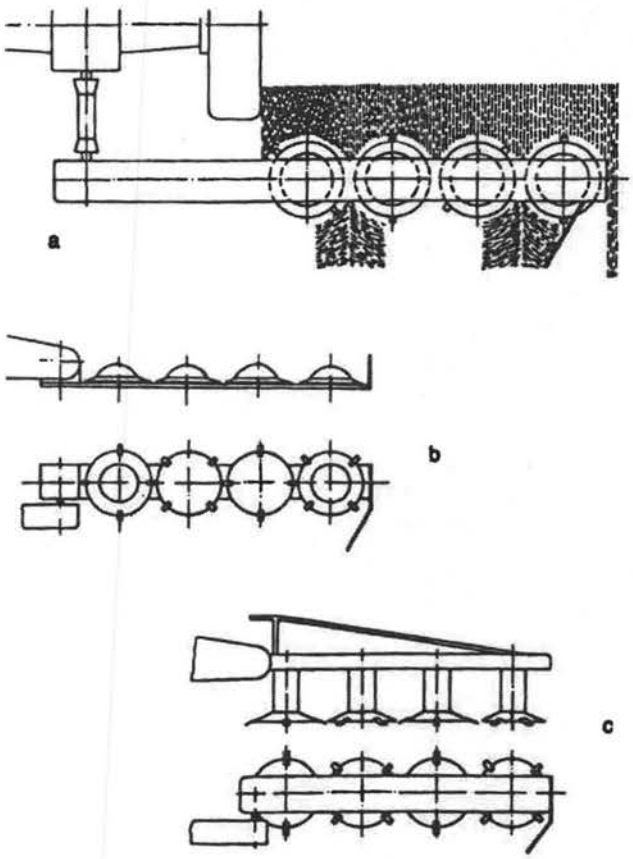

Figure 8.23–Rotary mowers, showing (a) cutting action, (b) disk-type mower, (c) drum-type mower (Reprinted form *Mechanics of Cutting Plant Materials*, Persson, 1987).

The power requirement of a flail mower is considerably higher than for a sickle bar mower of the same width, because impact cutting requires greater power than cutting with a countershear and because of the air pumping done by the rotor. Therefore, equation 8.12 is not valid for flail mowers because of the lack of a countershear. ASAE Data D497 suggests the following equation for calculating the power requirement of a flail mower mowing alfalfa:

$$P_{mow} = 8.2 + 2.13\ \dot{m}_f \qquad (8.24)$$

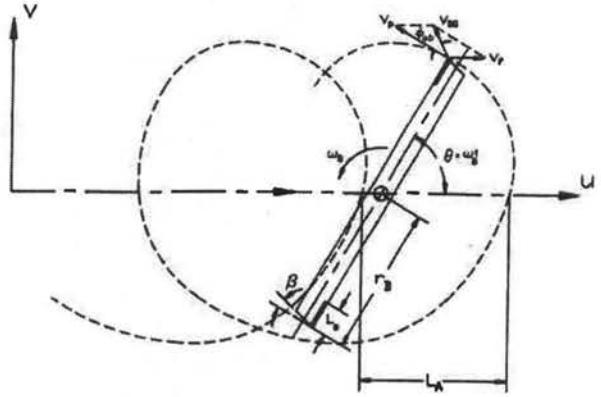

Figure 8.24–Analysis of cutting action of a rotary mower.

where

P_{mow} = pto power required for flail mower (kW)
$\dot{m}_f$ = feed rate (kg/s)

Drawbar power needed to overcome rolling resistance of the mower must be added to obtain the full power requirement. The feed rate of any mower can be calculated from the following equation:

$$\dot{m}_f = \frac{Y\, w_s\, v_f}{10} \tag{8.25}$$

where

Y = forage yield, wet basis (Mg/ha)
w_s = swath width cut by mower (m)
v_f = travel speed (m/s)

Combining equations 8.24 and 8.25 shows that, as expected, the power requirement increases with the speed and cutting width of the flail mower. Since the mower must convey the material (see fig. 8.21) as well as cut it, the power requirement also increases with crop yield. The power requirement with zero yield is an indication of the power needed for air pumping and to overcome friction in the mower.

Impact cutting, vertical axis. Figure 8.23, a rotary mower for mowing forage, is an example of impact cutting using a vertical axis. Figure 8.23b shows the disk-type mower in which the drive mechanism is below the cutting blades. In the drum-type mower shown in figure 8.23c, the drive is above the cutting blades and

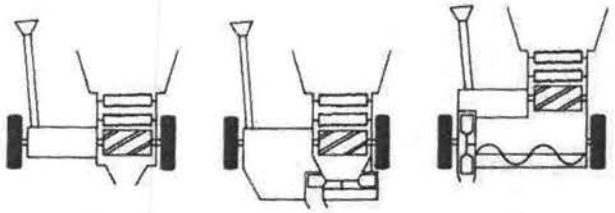

Figure 8.25–Forage harvesters with (a) cut and throw away delivery, (b) cut and blow delivery, (c) cut and blow with intermediate auger transport (Courtesy of Deere and Co.).

adjacent drums are counter-rotating so that the cut crop falls in distinct bands rather than being uniformly distributed across the cutting width. Mowers are also available in which all blades rotate in the same direction. Blades of adjacent disks or drums are designed to overlap to assure complete cutting. As each blade rotates about its center with velocity ω_b while the center moves forward with velocity v_f, the blade tip follows a cycloidal path over the ground (fig. 8.24). The velocity of a blade tip relative to the ground is the vector sum of the forward velocity and the peripheral velocity of a blade tip, i.e.:

$$v_{bg} = v_f + v_p \tag{8.26}$$

where

v_{bg} = velocity of blade tip relative to ground (m/s)
v_f = forward velocity of mower (m/s)
v_p = peripheral velocity of blade tip (m/s = $r_b \cdot b$)
r_b = radius out to blade tip (m)
ω_b = rotational speed of blade (rad/s)

Since the x-direction is defined as the direction of the blade relative to the material, it is in the direction of v_{bg} and constantly changes in direction as the blade rotates. In the nonrotating u,v coordinate system shown in figure 8.24, the mower moves in the u-direction. The u and v components of blade tip velocity are:

$$v_u = v_f - r_b \omega_b \sin(\omega_b t) \tag{8.27}$$

$$v_v = r_b \omega_b \cos(\omega_b t) \tag{8.28}$$

where

v_u = component of blade tip velocity in u-direction (m/s)
v_v = component of blade tip velocity in v-direction (m/s)
t = time (s) measured from point where $\theta = .$
θ = angle between blade and direction of travel = $\omega_b \cdot t$ (see fig. 8.24)

The oblique angle, ϕ_{ob}, can be calculated using the following equation:

$$\tan(\phi_{ob}) = \frac{1}{C_v \cdot \sec(\theta) - \tan(\theta)} \tag{8.29}$$

where $C_v = V_p/V_f$. If $v_f = 0$, then $\phi_{ob} = 0$. Since v_f is always much smaller than v_p, the oblique angle is always close to zero in a rotary mower and sliding of plant material along the blade is not a problem.

The crescent shaped area between two successive passes of a blade (fig 8.24) defines the area cut by each pass of a blade. The advance per blade, L_a, is given by:

$$L_a = \frac{2\pi v_f}{\lambda_b \omega_b} \tag{8.30}$$

where

L_a = advance per blade passage (m)
λ_b = number of blades on each disk or drum

The width of the sharpened ends of the blades, L_s, must be greater than L_a. Because the blade velocity must be high for impact cutting (see eq. 8.16) and the blade peripheral velocity declines toward zero at the center, L_a must be limited to assure reliable cutting. The permissible L_a would be considerably less than is shown in figure 8.24, where L_a was enlarged for clarity. To avoid crop drag against the ends of the blades (which are not sharpened), the ends must be tapered at angle β (see fig. 8.24). The most critical point for crop drag is at $\theta = 0$, when the blade is aligned with the direction of travel. The minimum required angle β is:

$$\beta = \arctan \frac{v_f}{r_b \omega_b} \tag{8.31}$$

The maximum width cut by each disk or drum is $2 \cdot r_b$ but, to assure complete cutting, some overlap is necessary and the disks or drums must be spaced less than the maximum cutting width. The drive provides timing such that knives on any disk (or drum) do not strike those on adjacent units. Example problem 8.4 illustrates design considerations for a vertical-axis mower.

Example Problem 8.4

In a rotary mower as shown in figure 8.23b, each disk carries four blades and rotates at 3000 rev/min. Each disk is to cut a 0.4 m swath. If the maximum travel speed is 15 km/h, calculate (a) the minimum required length of each knife. (b) Select an actual blade length, and (c) base diameter of each disk onto which the knives are to be attached. (d) Finally, calculate the minimum taper angle on the end of each blade.

Solution. (a) Equation 8.30 can be used to calculate the minimum length of each of the four blades on each disk. The travel speed is 15 km/h or 4.17 m/s; the disk rotation speed is 3000 rev/min or 314 rad/s. Then the minimum blade length is:

$$L_a = 2\,\pi\,4.17/(4 \cdot 314) = 0.021 \text{ m or } 21 \text{ mm}$$

(b) Such short blades would leave little room for accumulation of cut plants to be carried from the front to the side of the disk for discharge. Thus, we will select a longer blade length, 0.05 m or 50 mm. (c) The base disk diameter will then be:

$$\text{disk diameter} = 0.4 - 2 \cdot 0.05 = 0.3 \text{ m or } 300 \text{ mm}$$

(d) Equation 8.31 can be used to calculate the minimum taper of the ends of the blades:

$$\beta = \arctan\,[4.17/(0.2 \cdot 314)] = 3.8°$$

Several design features are included on rotary mowers for safety purposes. The knives are hinged to the disk or drum so that they can swing back if they hit a rock or other obstruction; centrifugal force keeps the knives in cutting position during normal operation. Since the rotating cutters have appreciable inertia, an over-running clutch is usually provided in the drive to allow the mower to coast to a stop when power is interrupted. When rocks are encountered, the high-speed knives are capable of launching them as projectiles that could injure the operator or bystanders. Thus, for safety reasons, the entire cutterbar is covered by a canvas or flexible plastic shroud.

The power requirement of a rotary mower is much higher than that of a sickle bar mower of the same width, because the forage is not only cut but also accelerated by the knives during impact. Tests at the NIAE, National Institute of Agricultural Engineering, (Persson, 1987, p. 176) in England suggest the following equation for calculating power requirements of a rotary mower:

$$P_{mt} = (P_{Ls} + E_{sc}\, v_f)\, w_c \tag{8.32}$$

where

P_{mt} = total pto power to mower (kW)
P_{Ls} = specific power losses due to air, stubble and gear-train friction (kW/m of width)
E_{sc} = specific cutting energy (kJ/m^2)
w_c = width of mower (m)

The NIAE data suggest that $1.5 < P_{Ls} < 4$ kW/m for disk and drum-type rotary mowers; disk mowers are at the lower end of the range, while drum mowers are at the upper end. Values of E_{sc} ranged from 1.5 kJ/m^2 for sharp blades to 2.1 kJ/m^2 for mowers with worn blades. A more recent survey of rotary mowers on the market indicated total pto power requirements ranging from 11 to 16 kW/m of cutting width while mowing at 15 km/h. Power to propel the mower and tractor must be added to obtain the total power requirement for mowing. Disks on typical mowers rotate at 3000 rev/min while cutting a 0.4 m swath per disk. Typical peripheral knife speeds are between 60 and 70 m/s. Mowers are available with from three to seven disks to provide a range of swath widths.

Chopping. Forage harvesters include means for gathering the crop into the machine, chopping it into short pieces and conveying the chopped forage into a wagon or truck. ASAE Standard S472 defines two basic types of forages harvesters, i.e., precision cut and nonprecision cut. A cylindrical cutterhead and stationary countershear are used for chopping in most precision-cut forage harvesters. Nonprecision-cut forage harvesters, to be discussed later, make use of a flail cutter for cutting and chopping the standing crop. Precision-cut forage harvesters can be further subdivided into cut-and-throw and cut-and-blow types. The cut-and-throw harvesters (fig. 8.25a) utilize energy imparted to the forage during cutting to transport the chopped material from the harvester. The cut-and-blow configuration (fig. 8.25b) uses an auxiliary blower for material transport. An auger conveyor is used between the chopper and blower on some forage harvesters (fig. 8.25c). The cut-and-blow

configurations allow the blower and wagon to be placed directly behind the tractor, thus eliminating side draft. The cut-and-throw configuration requires fewer components and can require less energy.

Three different types of headers are available for the precision-cut harvesters, i.e., direct-cut, windrow pickup, or row-crop headers (fig. 8.26). Direct-cut headers with widths up to 4.3 m include a reciprocating sickle and reel similar to those on combine harvesters (fig. 8.26a). Pick-up headers (fig. 8.26b) are for chopping haylage, i.e., forage that has been allowed to partially dry in the windrow. Row-crop headers (fig. 8.26c) with up to six-row capacity are used when maize or other row crops are to be chopped. Reciprocating sickles on earlier row crop headers have given way to a pair of rotating cutting disks for cutting each row. A pair of gathering chains, or a pair of fluted rubber gathering belts backed by roller chains, grab the cut stalks and pull them into the feed mechanism with the base of the stalks leading (fig. 8.27).

Figure 8.28 shows two types of feeding mechanisms for precision-cut forage harvesters. In either type, the upper feed rolls are spring-loaded to pre-compress the forage before it reaches the cylinder. The length of cut is controlled by the peripheral speed of the feed rolls relative to the speed of the cutterhead. A smooth feed roll is placed near the shear bar to maintain the grip on the forage as close to the shear bar as possible. In determining peripheral speeds of fluted feed rolls, the pitch (effective) diameter is slightly less than the outside diameter.

The theoretical length of cut can be calculated using the following equation:

$$L_c = \frac{60000\, v_f}{\lambda_k\, n_c} \tag{8.33}$$

where

L_c = theoretical length of cut (mm)
v_f = feed velocity (m/s = peripheral speed of feed rolls)
λ_k = number of knives on the cutterhead
n_c = rotational speed of cutterhead (rev/min)

Some particles will be longer than the theoretical length when stems are not oriented parallel to the direction of feed. Others will be shorter than the theoretical length when the arrival of the ends of stems does not coincide with the arrival of a cutterhead knife. Theoretical lengths of cut range from 3 to 90 mm. The actual length of cut is usually close to the theoretical length for row crops because the stalks are oriented nearly perpendicular to the shear bar. For

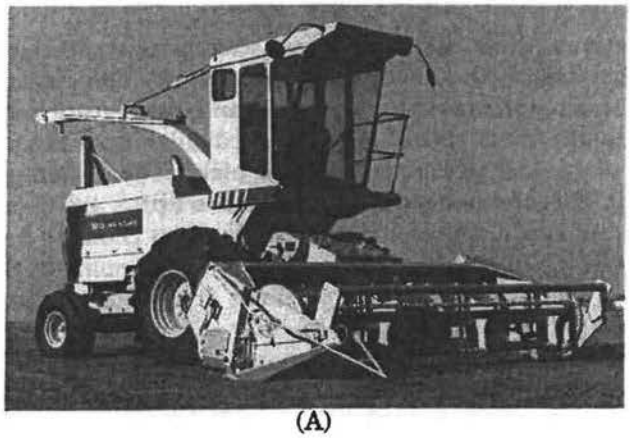

(A)

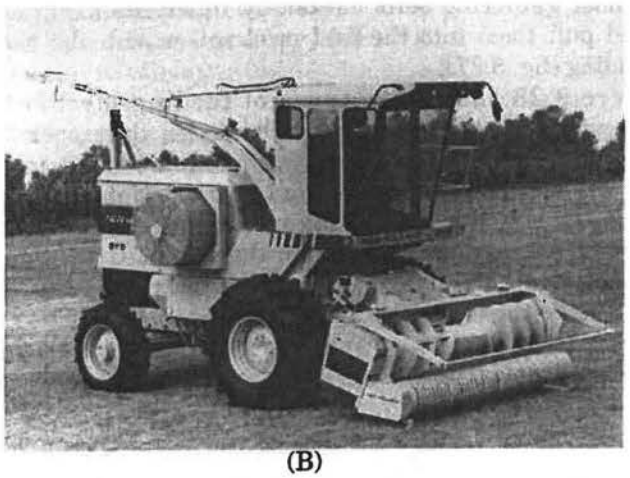

(B)

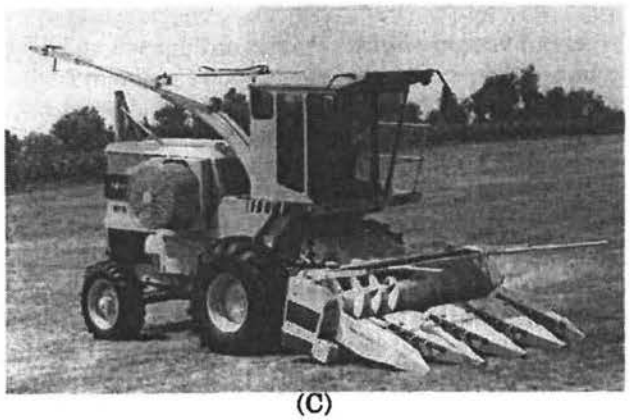

(C)

Figure 8.26–Gathering units for forage harvesters (Courtesy of New Holland, Inc.).

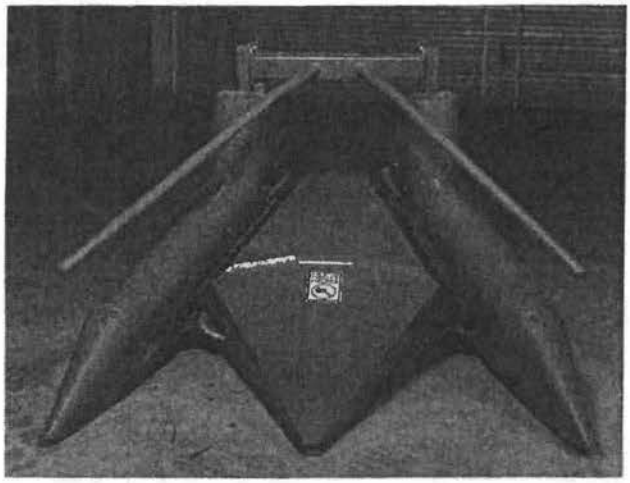

Figure 8.27–Rotary cut-off knives and gathering chains on a row unit of a forage harvester (Courtesy of Case-IH).

direct-cut forages, actual average lengths of cut are generally about 50% longer than the theoretical length. When windrowed crops are being chopped, the average actual length of cut is much longer than the theoretical length due to the random stem alignment. On a specific forage harvester, large increases in theoretical length of cut are made by removing knives from the cutterhead. For example, by going from 12 to 6 to 3 knives, the length of cut can be doubled twice. Another popular pattern is 8 to 4 to 2 knives. Smaller changes in length of cut are made by adjusting the feed velocity. The feed rolls will separate further to accommodate the reduced feed velocity until the maximum separation distance is reached; further reductions in feed velocity will then reduce the capacity of the harvester. The cutterhead speed is normally maintained at its maximum design value, typically 850 to 1000 rev/min, and thus is not adjusted.

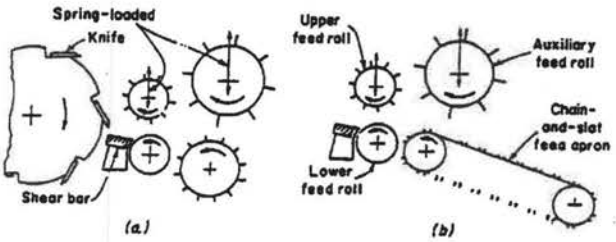

Figure 8.28–Two types of feed mechanisms for a forage harvester (Reprinted from *Principles of Farm Machinery*, Kepner et al., 1978).

Cutterhead diameters normally range from 520 to 770 mm and widths range from 450 to 620 mm.

The theoretical capacity of a precision-cut forage chopper can be calculated using the following equation:

$$\dot{m}_f = \frac{\rho_f A_t L_c \lambda_k n_c}{6 \times 10^8} \tag{8.34}$$

where

$\dot{m}_f$ = theoretical capacity or feed rate (kg/s)
ρ_f = density of forage in the throat (kg/m^3)
A_t = throat area (cm^2)

Throat areas vary considerably among forage harvesters, but usually are within the range from 770 to 1350 cm^2. Based on research at the University of Wisconsin, typical forage densities between the feed rolls range from 56 kg/m^3 for hay at 26% moisture to 340 kg/m^3 for green corn (maize). If the forage yield changes during any given pass through a field, the corresponding change in capacity is accommodated through changes in the depth of forage between the feed rolls. Thus, the top feed rolls must be spring loaded to permit such changes in depth. The throat area is equal to the product of cylinder width times maximum forage depth between the upper and lower feed rolls. Maximum depths are typically in the range from 140 to 180 mm.

After the forage is chopped by the cutterhead, centrifugal force holds it against the housing as the cutterhead moves it toward the exit; the housing terminates at the bottom or rear of the cutterhead to allow the chopped material to escape. In a cut-and-throw machine, the cutterhead imparts sufficient energy to throw the chopped material to a trailing wagon or truck. Alternatively, in a cut-and-blow machine, a separate impeller-blower is used to convey the chopped material. Sometimes a recutter screen is installed at the exit of the cutterhead housing. Working against the recutter screen, the cutterhead further reduces the average length of cut of the exiting material (fig. 8.29). On machines with a recutter, an impeller-blower must be used to convey the chopped material. Electric motors or a hydraulic actuator controllable from the operator's seat permit swiveling the spout and/or tipping the end deflector to direct the forage to completely fill the truck or wagon (fig. 8.30). Figure 8.29 illustrates one method for providing access to the cutterhead and recutter screen. The impeller-blower is hinge-connected to the forage harvester. Swinging the impeller-blower away from the cutterhead

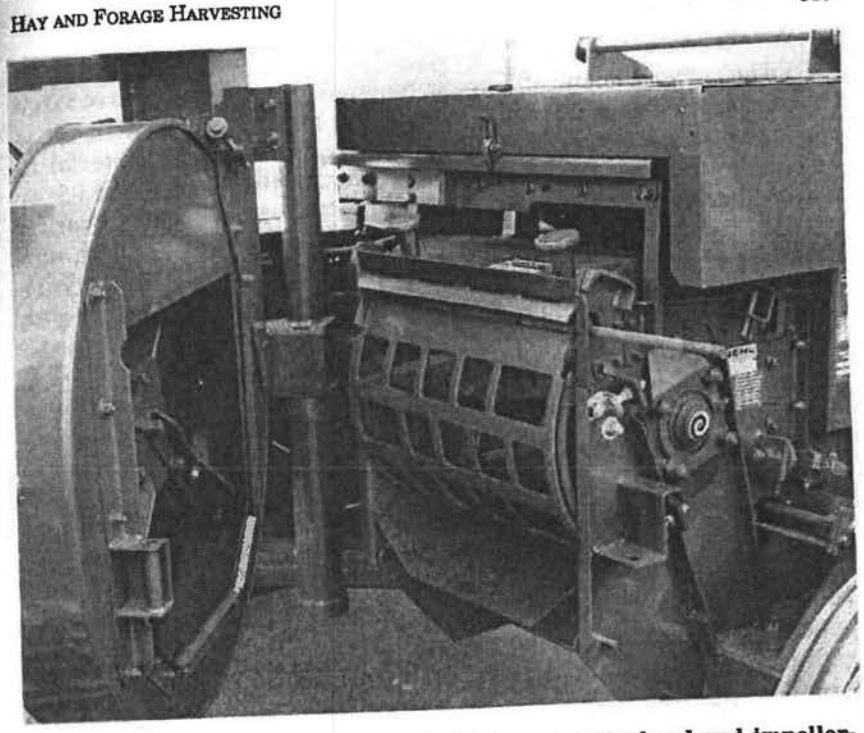

Figure 8.29–Recutter screen installed between cutterhead and impeller-blower (Courtesy of Gehl Equipment Co.).

permits access for installing or removing a recutter screen or for servicing the cutterhead.

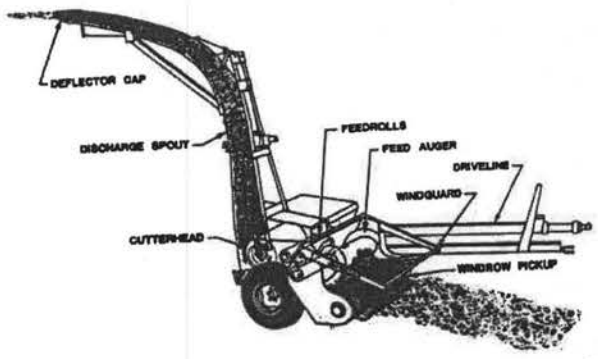

Figure 8.30–Rear view of a forage harvester showing adjustable discharge spout and deflector cap (Courtesy of Prairie Agricultural Machinery Institute, Canada).

The power demand of a precision-cut forage harvester is so large that harvesting capacity can be limited by available power. Power is consumed in gathering, conveying and compressing the material to be cut, in chopping the material and in conveying it to the truck or wagon. Parasitic power losses in a forage harvester include bearing friction, friction of the cut material on the cutterhead housing, and pumping of air at the cutterhead and blower. Numerous researchers have found that power use in cut-and-blow forage harvesters can be divided roughly as follows: 20% to gathering and feeding, 40% to the cutterhead, and 40% for blowing. Within the cutterhead, energy is required for compressing and shearing, for acceleration and air movement, and for overcoming friction at the housing. Within the blower, energy is required for acceleration, for air movement and for overcoming friction. Material parameters such as shear strength, moisture content and friction coefficient, and machine parameters such as sharpness of the knife and length of cut will all affect the distribution of power in the harvester. However, cutting usually requires the greatest energy at the cutterhead, while friction generates the greatest energy requirement at the blower. The power requirement for chopping can be calculated using the following equation:

$$P_c = \frac{1000\, C_f F_{smax} \dot{m}_f}{\rho_f L_c} \tag{8.35}$$

where

P_c = power required for chopping (kW)
$\dot{m}_f$ = feed rate (kg/s)
ρ_f = density of material in throat (kg/m^3)
L_c = theoretical length of cut (mm)
F_{smax} = maximum specific cutting force (N/mm of countershear length)
C_f = ratio of average to maximum specific cutting force

The knives on the cutterhead in forage harvesters are normally helix-shaped; the resulting oblique cutting extends the duration of each cut while reducing the peak cutting force. Compared to the force-displacement diagram for a straight cut (fig. 8.15), oblique cutting would lengthen and lower the diagram without changing the area under the curve. Thus, as with straight cutting, C_f is about equal to 0.64 for typical oblique cutting. Power for chopping varies with feed rate and length of cut; the specific cutting energy provides a better index for comparing forage harvesters of differing design. Specific cutting energy is defined as follows:

$$E_{sc} = \frac{1000\, C_f F_{smax}}{\rho_f} \tag{8.36}$$

where E_{sc} = specific cutting energy per unit mass on the countershear (J·m/kg)

By measuring power consumption while changing feed velocity and removing knives to change the theoretical length of cut and by assuming that such changes did not change other power requirements in the forage harvester, Richey (1958) estimated the specific energy requirements of two cylindrical cutterheads. For those tests, chopping alfalfa at 73% moisture and a 13-mm length of cut consumed 0.33 kW·h/Mg, giving a value of E_{sc} = 15.4 J·m/kg. Once a value of E_{sc} is known, the following equation can be used to calculate power:

$$P_c = \frac{E_{sc}\, \dot{m}_f}{L_c} \tag{8.37}$$

Notice from equation 8.36 that E_{sc} is proportional to the maximum specific cutting force. Thus, maintaining sharp knives and shearbar/knife clearance is very important to reduce the power requirement for forage chopping. As the knife edge wears from a 0.1 mm (sharp) to a 0.3 mm radius (dull), the cutting energy approximately doubles. The cutting energy also doubles as the clearance increases from 0.1 to 0.4 mm. The combined effect of dulling the knife and increasing the clearance as indicated above is approximately a tripling of the cutting energy. Dull knives and excessive clearance cause the crop to be torn rather than sheared and also accelerates wear due to wedging between the knife and shearbar. A sharpening stone with automatic traversing along the cutterhead is included as a standard feature of many forage harvesters. The automatic sharpener permits the operator to interrupt harvesting and sharpen the knives without leaving the field. The clearance should also be easy to adjust. The adjustment must be done with the cutterhead running at normal speed to accommodate the centrifugal expansion of the cutterhead.

Metal detectors are another valuable option on forage harvesters. Metal can damage the chopper and/or kill livestock that consumes the metal in the forage. When a magnetic sensor detects metal in the throat, the feed rolls are automatically stopped to prevent the metal from reaching the cutterhead. The feed rolls must be reversed to expel the metal-bearing forage before harvesting can be resumed.

Power to overcome friction between the cut forage and the cutterhead or blower housing can be calculated by using the following equation:

$$P_f = \frac{\beta \mu \dot{m}_f v_{pc}^2}{1000} \tag{8.38}$$

where

P_f = power absorbed by rubbing friction (kW)
β = average arc of housing rubbed by chopped material (radians)
μ = coefficient of friction between forage and steel housing
$\dot{m}_f$ = feed rate (kg/s)
v_{pc} = peripheral velocity of cutterhead (m/s)

Material leaving the cutterhead does not all strike the housing at the same place, so angle β is the average angle of contact. Manufacturers have realized that a short cutterhead housing is desirable to reduce friction power and thus have minimized arc β in most modern forage harvesters. ASAE Data D251 presents data on friction coefficients between chopped forages and metal surfaces. Friction coefficients for forage on steel range from 0.2 to 0.8 depending on type of forage, moisture content, peripheral velocity and other factors. Peripheral velocities of cutterheads typically range from 20 to 28 m/s and, for such velocities, both chopped corn and chopped alfalfa have a coefficient of approximately 0.49 on polished stainless steel.

Power required to accelerate the forage at the cutterhead or blower is derived by assuming that the forage leaves the blades at about the peripheral speed of the blades:

$$P_{accel} = \frac{\dot{m}_f v_{ip}^2}{2000} \tag{8.39}$$

where

P_{accel} = power to accelerate the forage (kW)
v_p = peripheral velocity of the cutter or blower (m/s)

Both the cutterhead and the blower move air, although the latter at a greater rate. According to well-established fan laws, fan power varies with the cube of the peripheral speed. Making use of data by Blevins

and Hansen (1956), the following equation was derived for the approximate air power:

$$P_{air} = \frac{v_p^3}{16{,}600} \tag{8.40}$$

where P_{air} = power to move air (in kW).

The header power, including power for the feed rolls, varies with the feed rate and is not large except at very high feed rates. The following equation can be used to estimate the header power:

$$P_h = C_{h0} + C_{h1}\,\dot{m}_f \tag{8.41}$$

where

P_h = power consumed by header (kW)
C_{h0}, C_{h1} = constants for any given header (kW and kW·s/kg)

C_{h0} is the amount of power required to overcome friction when the harvester is running empty. Cutting, conveying and compressing the forage between the feed rolls absorbs power in proportion to the feedrate.

By combining equations 8.36 and 8.38 through 8.41, an equation for the total power consumption, P_{fh}, of a forage harvester can be obtained. Note that air power is independent of feed rate, but power to all other components is proportional to feed rate. The form of the equation for P_{fh} is thus similar to the following equation from ASAE Data D497 for the total power consumption of a precision-cut forage harvester:

$$P_{fh} = 1.5 + 3.3\,C_r\,C_c\,\dot{m}_f \tag{8.42}$$

where

P_{fh} = total power consumed by forage harvester (kW)
C_r = recutter factor = 1.0 for no recutter or 2.0 with recutter screen
C_c = crop factor = 1.0 for green corn, 1.33 for green alfalfa or 2.0 for low-moisture forage or hay

Although equation 8.42 has the proper form, the constants in it represent only average conditions and the equation is not useful for

exploring the effect of various design variables. The design of a precision forage harvester is illustrated in example problem 8.5.

Example Problem 8.5

A cut-and-throw forage harvester has a cylindrical cutter head with width of 500 mm and diameter of 600 mm carries eight knives and rotates at 950 rev/min. The average length of cut is to be 7 mm. The maximum height of the throat is 18 cm. When cutting corn, the compressed density of material in the throat is 320 kg/m^3, and the specific cutting energy is 15 J·m/kg. The coefficient of friction between the forage and the housing is 0.49, and the material is in contact with the housing through 2.5 radians of arc. Assume the power coefficients for the header are 0.6 kW and 0.3 kW·s/kg. Calculate (a) the required feed velocity into the cutterhead, (b) the maximum allowable feedrate into the harvester and (c) the total power requirement of the harvester.

Solution. (a) The required feed velocity can be calculated by solving equation 8.33 for v_f:

$$v_f = L_c \lambda_k n_c/60\,000 = 7 \cdot 8 \cdot 950/60\,000 = 0.887 \text{ m/s}$$

(b) Before using equation 8.34 to calculate the maximum allowable feedrate, the maximum throat area must be calculated. It is:

$$A_t = \text{cutterhead width} \cdot \text{throat height} = 50 \cdot 18 = 900 \text{ cm}^2$$

Then the maximum allowable feedrate is:

$$\dot{m}_f = 320 \cdot 900 \cdot 7 \cdot 8 \cdot 950/(6 \times 10^8) = 25.5 \text{ kg/s or } 92 \text{ Mg/h}$$

(c) The various component power requirements must be calculated using equations 8.37 through 8.41 to get the total power requirement. The peripheral velocity of the cutterhead is needed to calculate the power used in friction, in accelerating the forage and in moving air. The radius of the cutterhead is 0.3 m and the rotation speed is 99.5 rad/s. Then the peripheral velocity is:

$$v_{pc} = v_{pi} = 0.3 \cdot 99.5 = 29.9 \text{ m/s}$$

Now the various power requirements can be calculated:

$$P_c = 15 \cdot 25.5/7 = 54.6 \text{ kW}$$

$$P_f = 2.5 \cdot 0.49 \cdot 25.5 \cdot 29.9^2/1000 = 27.9 \text{ kW}$$

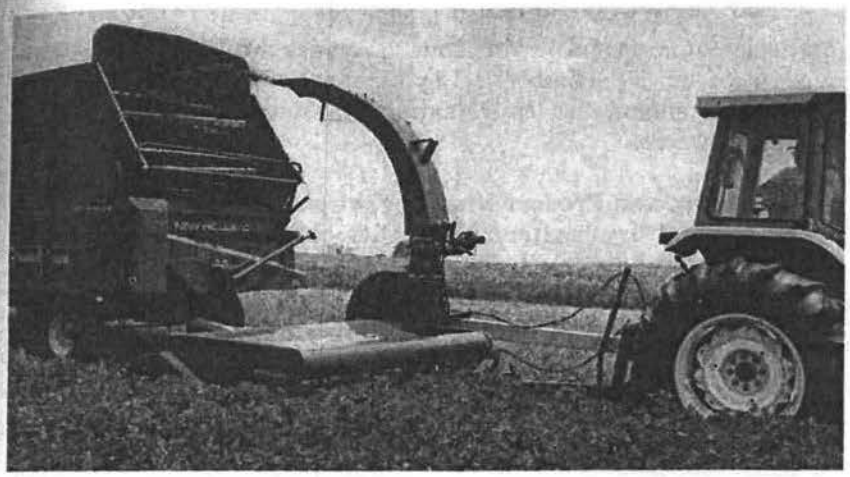

Figure 8.31–A flail-type forage harvester (Courtesy of Ford New-Holland, Inc.).

$$P_{accel} = 25.5 \cdot 29.9^2/2000 = 11.4 \text{ kW}$$

$$P_{air} = 29.9^3/16600 = 1.6 \text{ kW}$$

$$P_h = 0.6 + 0.3 \cdot 25.5 = 8.3 \text{ kW}$$

$$P_{fh} = 54.6 + 27.9 + 11.4 + 1.6 + 8.3 = 103.8 \text{ kW}$$

In this example of a cut-and-throw harvester, the power delivered to the shaft of the cutterhead would be the sum of P_c, P_f, P_{accel}, and P_{air}. Thus, 95.5 kW, or 92% of the total power requirement would be delivered to the shaft of the cutterhead.

Forage harvesters with nonprecision cut represent a lower-cost alternative to precision-cut harvesters. Figure 8.31 shows a flail-type forage harvester, which has a nonprecision cut. Flails similar to those in a flail mower (fig. 8.21) cut the standing crop and deliver it into a cross auger. Rotor speeds are usually in the range from 1100 to 1600 rev/min, giving flail peripheral speeds in the range from 45 to 60 m/s. The auger conveys the cut forage to an impeller-blower to be conveyed to the trailing wagon. On some flail harvesters, a flywheel-type cutterhead is substituted for the impeller-blower. The cutterhead recuts the forage and conveys it to the wagon. Recutters generally have two, three, or six knives to provide varying lengths of cut. The average recut lengths are comparable to those from precision-cut forage harvesters except that the lengths are less uniform. Power requirements of a flail-type forage harvester with recutter are typically double or greater compared to those of a

precision-cut forage harvester. Thus, the lower initial cost of the flail-type harvester is partially offset by higher operating costs. The flail-type harvesters are also less versatile because they cannot be used to harvest row crops.

8.2.3 Curing and Preservation of Forage

Losses of dry matter and quality can be very large during harvest of hay, especially for leafy hay such as alfalfa or other legumes. In alfalfa, for example, crude protein accounts for about 28% of the leaf dry matter but only 11% of the stem dry matter. Protein and nonstructural carbohydrates provide most of the nutritional value from the forage; NDF (nondetergent fiber) is less digestible and serves primarily as roughage (a coarse substance, usually high in cellulose, whose bulk stimulates peristalsis in the intestines). Dry matter and quality losses occur due to plant respiration, rain, and machine losses during harvesting. Typically, 3 to 5% of the plant dry matter, consisting primarily of nonstructural carbohydrate, is lost through respiration after cutting. Respiration losses thus increase the concentration of crude protein and NDF in the forage. Respiration ceases when the plants dry to 40% moisture. Rain causes leaf shatter and leaching losses. Leaf losses readjust the leaf to stem ratio, resulting in an overall loss in crude protein concentration and increased fiber concentration. Leaching losses from both leaves and stems consist of nonfiber; the leaching loss of crude protein is typically 20% greater than leaching loss of other dry matter. Machine losses include both leaves and stems but leaves are lost more readily; thus the reduction in the leaf-stem ratio caused by machines can reduce the overall protein concentration in the forage. Since fast drying of forage reduces respiration losses and also the opportunity for rain to fall on the cut forage, losses of both dry matter and quality are decreased by faster drying.

Leaves of legume crops dry much faster than the stems because the surface-volume ratio of leaves is much greater than that for stems. Also, a waxy cutin layer on the surface of stems acts as a natural moisture barrier and reduces their drying rate. Conditioning is a process in which the stems are crushed, cracked or abraded such that they dry at approximately the same rate as the leaves. Magnified cross-sections of conditioned and unconditioned stems is shown in figure 8.32. Conditioning of legumes is usually accomplished by running the forage between a set of rolls, either of the corrugated crimper type or the intermeshing crushing type. The corrugated crimper, which has deep flutes that feed aggressively, is less likely to plug but can cause excessive leaf loss. Conditioning occurs through splitting each stem as it is bent to pass through the rolls. Intermeshing crushing rolls are less aggressive and thus less

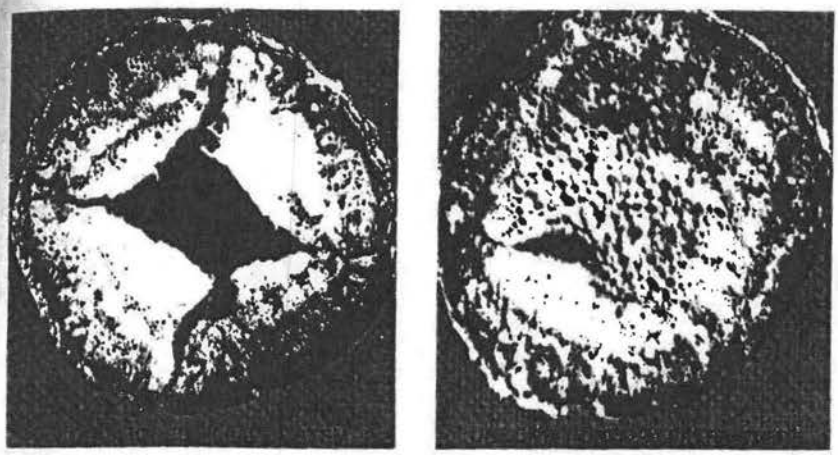

Figure 8.32–Magnified compression of conditioned and unconditioned alfalfa stems (Courtesy of Deere and Co.).

likely to cause leaf loss. Conditioning is accomplished by crushing the stems. The peripheral speed of conditioners should be three to four times the travel speed of the machine to maintain a thin layer of forage between the rolls, since thin layers are conditioned more effectively and uniformly than thick layers. Thin layers are also facilitated when the reel provides a uniform feed rate to the conditioner and by use of the widest possible rolls; however, stiffness limitations place a practical limit on roll width. Roll spacing must automatically vary to accommodate different crop yields. Springs are used to maintain pressure between the rolls and the spring force is adjustable to control the degree of conditioning. An adjustable minimum clearance is also provided between the rolls; minimum clearance is increased for crops with larger stems, since excessive roll pressure or insufficient clearance can cause excessive leaf loss. Rolls are usually constructed from steel, neoprene or tire carcasses. Shinners et al. (1990) found no difference in leaf loss or drying rate of alfalfa due to type of rolls.

Using conventional techniques for harvesting, hay curing in the field required from three to five days depending on weather conditions. Use of crop conditioners to crush the stems (fig. 8.5) accelerated the drying and reduced curing time to two to four days. Use of chemical agents to accelerate drying of crushed hay can reduce curing time by an additional day. Spraying an aqueous solution of potassium and/or sodium carbonate on the forage increases the permeability of the waxy cutin surface of the plants, thus allowing faster escape of moisture (Rotz et al., 1990). A recent

technique, in which alfalfa is shredded and pressed into a mat, may allow alfalfa to cure in as little as four hours (Rotz et al., 1990).

A model of drying of swathed alfalfa was developed by Rotz and Chen (1985); drying dynamics may differ when the swath is raked. For the swathed alfalfa, Rotz and Chen found that two environmental factors predominate in driving the drying process; solar radiation provides the energy for moisture evaporation, while the vapor pressure deficit provides the moisture gradient to move the water vapor away from the plants. The two most important variables which limited the drying rate were swath density and soil moisture. Drying theory shows that, as material density approaches infinity, the drying rate approaches zero. Drying is also slowed when soil moisture keeps a wet surface at the bottom of the swath. The equilibrium moisture content is an important variable in drying theory. However, the model of Rotz and Chen best described actual drying when the equilibrium moisture content was assumed to be zero. Then the following equation gives the moisture content at any time during daylight drying:

$$M_f = M_{fo}\, e^{-C_{dr}\, t} \tag{8.43}$$

where

M_f = moisture content (dry basis) at end of time t
M_{fo} = moisture content (dry basis) at t=0
t = drying period (h)
C_{dr} = drying rate constant (1/h)

On the basis of 5000 experimental observations on the drying of alfalfa, the following two empirical equations were developed for the drying rate constant:

$$C_{dr} = \frac{S_{rad}(1 + 9.30\, R_c) + 5.42\, \Theta_{db}}{66.4\, M_s + \rho_s (2.06 - 0.97\, \lambda_d)(1.55 + 2.19 R_c) + 3037} \tag{8.44}$$

or,

$$C_{dr} = \frac{S_{rad}(1 + 9.03\, R_c) + 43.8\, p_{vd}}{61.4\, M_s + \rho_s (1.82 - 0.83\, \lambda_d)(1.68 + 24.8 R_c) + 2767} \tag{8.45}$$

where

S_{rad} = solar radiation (W/m^2)
R_c = application rate of chemical drying agent or conditioner (g of solution/g of dry matter)

M_s = soil moisture content (dry basis, %)
ρ_s = swath density (g/m^2)
λ_d = one on day of cutting, else 0
Θ_{db} = dry bulb temperature (° C)
p_{vd} = vapor pressure deficit (kPa)

The above equations apply only to daytime drying; rewetting by rain or dew will slow the drying process. Both models gave realistic prediction of alfalfa daytime drying rates in the East Lansing, Michigan, area and also in the semi-arid regions of California; the models have not yet been validated for other areas. Solar insolation rates typically range from 0 to 950 W/m^2. It is easier to measure dry bulb temperature than vapor pressure deficit and thus equation 8.44 may be best in areas of relatively high relative humidity. In very dry areas, equation 8.45 may give more realistic predictions of drying rate of alfalfa. The factor, λ_d, is in the model because drying is faster on the day of cutting when the moisture is still uniformly distributed through the swath. The top of the swath dries first and later moisture removal from the bottom of the swath occurs more slowly. Swath densities range from 150 to 1500 g/m^2, with 450 g/m^2 being a typical value. Note that the model makes no reference to the concentration of chemicals in the drying solution; tests have shown that the effectiveness was nearly independent of the concentration of the chemicals in the solution but was very dependent on the rate at which the solution was applied to the forage. Rates range from 0 to 0.25 grams of solution per gram of forage dry matter, with 0.075 g/g being a typical rate. Higher rates provide more complete coverage of the plant surfaces and thus promote drying. Example problem 8.6 illustrates the calculation of alfalfa drying.

Example Problem 8.6

On a day when the dry bulb temperature is 20° C, the solar radiation is 650 W/m^2, and the soil moisture is 18%, alfalfa is cut at 80% moisture in a humid area. The density of alfalfa in the swath is 450 g/m^2. Potassium carbonate drying agent is applied at the rate of 0.075 g/g. Calculate the moisture content of the hay at the end of the first hour and at the end of the second hour.

Solution. The hay was cut in a humid area and thus, from equation 8.44, the drying rate constant is:

$$C_{dr} = \frac{650\,(1 + 9.3 \cdot 0.075) + 5.42 \cdot 20}{66.4 \cdot 18 + 450\,(2.06 - 97 \cdot 1)\,(1.55 + 2.19 \cdot 0.075) + 3037} = 0.234$$

Then, from equation 8.43, the crop moisture at the end of the first hour is:

$$M_f = 89\ e^{-0.234 \cdot 1} = 63.3\%$$

At the end of the second hour, the crop moisture is:

$$M_f = 63.3\ e^{-0.234 \cdot 1} = 50.1\%$$

Thus, the forage lost 16.7 points of moisture in the first hour and 12.6 points in the second hour. Since the moisture loss during any hour is proportional to the beginning moisture, the hourly moisture loss continues to decline as the forage dries.

8.2.4 Windrowing

In some methods of forage harvesting, the forage is formed into windrows which can then be picked up directly by the harvester. This is common practice when harvesting forage for silage or where the climate is very dry. When dry hay is desired in humid climates, the forage is placed in a swath and then raked into a windrow. When cutting and windrowing are done in two separate operations, a side-delivery rake can be used to roll the swaths left by the mower into windrows. Rakes can also be used to invert previously-formed windrows to promote faster drying, especially after rain has wetted the windrows. Dry matter losses during raking typically range from 3 to 6% and more leaves than stems are usually lost. Thus, gentle handling is an important goal in rake design. The two most popular types of side delivery rakes are the oblique-reelhead rake and the finger-wheel rake.

A parallel bar (oblique-reelhead) rake is illustrated in figure 8.33. The two reelheads are parallel but at an acute angle with the tooth bars. Thus, when one of the reelheads is driven, either by pto power or by a ground wheel, every rake tooth follows a circular path in a plane parallel to the reelheads. All teeth automatically maintain parallel positions, usually vertical, but the pitch of the teeth can be changed by changing the tilt of the reelhead axes. Pitching the bottoms of the teeth forward gives a more vigorous raking action in heavy crops.

Figure 8.33 was used in deriving velocity relationships for a parallel-bar rake. Rake teeth contact the hay at angle α_1 from the lowest tooth position and release it at angle α_2 at the top of the windrow. Teeth are in contact with the hay during forward travel x_1 and out of contact during forward travel x_2. One expression for x_2 can be derived from figure 8.33b, i.e.:

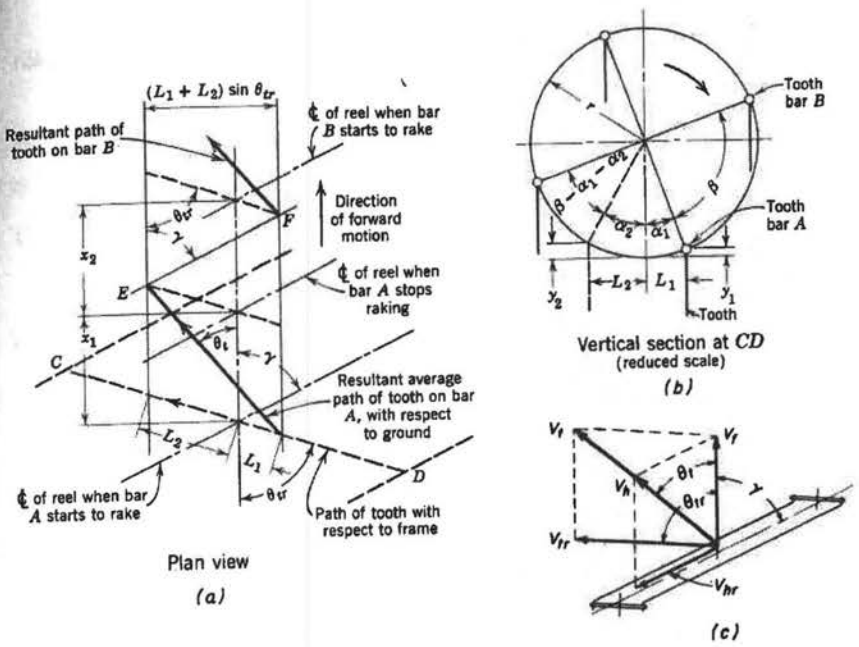

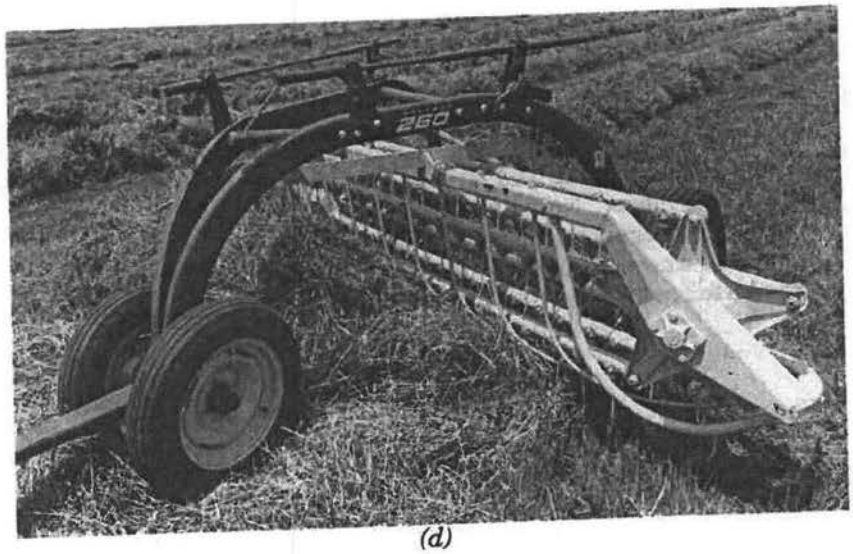

(d)

Figure 8.33–A side delivery rake with oblique reel-head (Courtesy of Ford-New Holland, Inc.).

$$x_2 = (L_1 + L_2)\left(\cos\theta_{tr} + \frac{\sin\theta_{tr}}{\tan\gamma}\right) \tag{8.46}$$

Another expression for x_2 can be derived from figure 8.33a, i.e.:

$$x_2 = r\frac{v_f}{v_p}\cdot(\beta - \alpha_1 - \alpha_2) \tag{8.47}$$

Then, since $L_1 = r\sin(\alpha_1)$ and $L_2 = r\sin(\alpha_2)$, equations 8.46 and 8.47 can be combined into the following equation:

$$\frac{\beta - \alpha_1 - \alpha_2}{\sin\alpha_1 + \sin\alpha_2} = \frac{v_p}{v_f}\left(\cos\theta_{tr} + \frac{\sin\theta_{tr}}{\tan\gamma}\right) \tag{8.48}$$

All terms in equation 8.47 are design variables except α_1 and α_2, which are unknowns depending upon operating conditions. From figure 8.33b:

$$\alpha_2 = \arccos\left(1 - \frac{y_2}{r}\right) \tag{8.49}$$

Distance y_2 can be determined as the height of the top of the windrow relative to the lowest position of the rake teeth. Then equation 8.49 can be solved for α_2 and equation 8.48 can be solved (iteratively) for α_1. Note that α_1 can be negative if the effective raking stroke begins beyond the lowest point of tooth travel. After α_1 and α_2 are known, the magnitude of vector v_{tr} can be calculated using the following equation:

$$\frac{v_{tr}}{v_p} = \frac{\sin\alpha_1 + \sin\alpha_2}{\alpha_1 + \alpha_2} \tag{8.50}$$

The direction of v_{tr} is parallel to the planes of the reelheads. After vector V_{tr} is determined, the direction and magnitude of v_t can be calculated. Angle θ_t can be calculated from:

$$\theta_t = \arctan\frac{v_{tr}\sin\theta_{tr}}{v_f + v_{tr}\cos\theta_{tr}} \tag{8.51}$$

and the magnitude, v_t can be calculated from:

$$v_t = \frac{v_{tr} \sin \theta_{tr}}{\sin \theta_t} \tag{8.52}$$

The direction of v_h is coincident with v_t. The magnitude of v_h can be calculated using the following equation:

$$v_h = \frac{v_f}{\cos \theta_t + \sin \theta_t + \text{cotan } \gamma} \tag{8.53}$$

The theoretical maximum distance travelled by the hay during raking is given by the following equation:

$$L_h = \frac{w_r}{\sin \theta_t} \tag{8.54}$$

Definitions of symbols in equations 8.46 through 8.54 are as follows:

- α_1 = angle before bottom at which raking begins (radians) (see fig. 8.33)
- α_2 = angle at which raking ends (radians)
- β = angle between tooth bars (radians)
- γ = acute angle between raking front and direction of travel (radians)
- θ_{tr} = angle between direction of travel and planes of reelheads (radians)
- θ_t = angle between v_t and direction of travel (radians)
- x_2 = horizontal distance travelled by teeth during nonraking (m)
- y_2 = vertical distance from lowest position of rake teeth to top of windrow (m)
- L_1+L_2 = horizontal distance travelled by teeth during raking (m)
- r = reel radius (m)
- v_f = forward velocity of rake (m/s)
- v_{tr} = reel component = average horizontal velocity of teeth during raking, relative to rake (m/s)
- v_p = peripheral speed of reel (m/s)
- v_t = resultant tooth velocity = vector sum of v_f and v_{tr} (m/s)
- v_{hr} = average horizontal velocity of hay relative to rake (m/s)
- v_h = average resultant hay velocity = vector sum of v_f and v_{hr} (m/s)
- L_h = maximum theoretical distance travelled by hay during raking (m)
- w_r = width of rake (m)

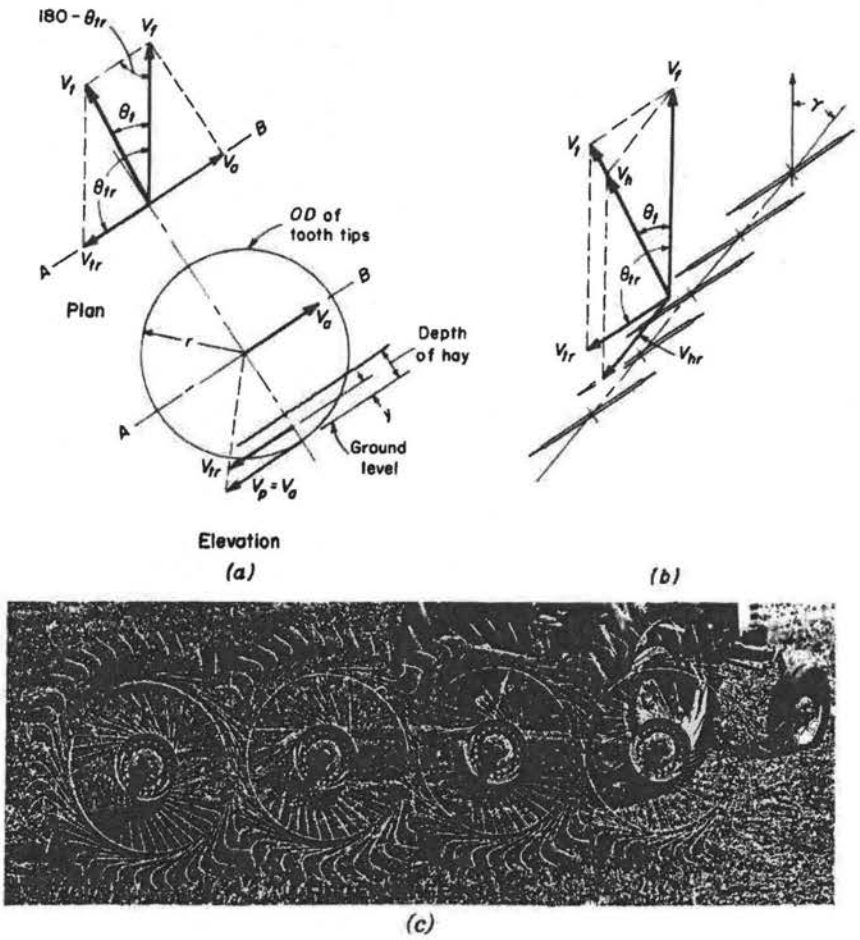

Figure 8.34–A finger-wheel side delivery rake (Courtesy of Deere and Co).

A finger-wheel side-delivery rake is illustrated in figure 8.34. The action of one raking wheel is illustrated in figure 8.34a, while velocity relationships for the complete rake are shown in figure 8.34b. Raking teeth are carried on wheels whose planes of orientation allow each wheel to be ground driven. Thus, no separate drive train is required. As was true for the oblique-reelhead rake, the vector v_{hr} is parallel to the raking front and v_{tr} is parallel to the planes of the raking wheels.

Since the tooth wheels are each ground driven, the magnitude of v_p can be calculated from the following equation (see fig. 8.34a):

$$\frac{v_p}{v_f} = \cos(\pi - \theta_{tr}) = \cos \theta_{tr} \tag{8.55}$$

The reel component, v_{tr}, is proportionally less than v_p as shown in the following equation:

$$v_{tr} = \frac{r - y}{r} v_p \tag{8.56}$$

where

y = half of the windrow height (m) (see fig. 8.34a)
r = radius from center of tooth wheels to tooth tips (m)

The angle, θ_t of the resultant tooth and hay path is given by the following equation:

$$\theta_t = \arctan \frac{v_{tr} \sin \theta_{tr}}{v_f} \tag{8.57}$$

The magnitudes of v_t and v_h can be calculated using equations 8.52 and 8.53, respectively. The theoretical maximum length of hay travel for the finger wheel rake can be calculated using equation 8.54.

The gentleness with which the hay is handled during raking is influenced by rake design variables. Gentleness is promoted by maintaining low hay velocity, v_h, by keeping v_t as close as possible to v_h to reduce tooth impacting on the hay, and by keeping hay travel, L_h, as small as possible. The ratio of v_h/v_t is closer to unity for the finger-wheel rake, thus providing a smoother raking action than for the parallel-bar rake. However, the finger-wheel rake has a somewhat longer hay path (compare figs. 8.33c and 8.34a). For the parallel-bar rake, reducing the ratio v_p/v_f lengthens the hay path but reduces the frequency of tooth impacts on the hay and also reduces the ratio v_t/v_h. Reducing v_f also provides gentler handing of the hay but decreases the raking capacity. The theoretical effects of the various raking parameters were determined analytically, but there is little published information on the effect of raking parameters on losses. Example problem 8.7 illustrates calculations for a side delivery rake with oblique reel head.

Example Problem 8.7

A five-bar side delivery rake with an oblique reel head has a raking front angle, $\gamma = 65°$ (6.81 rad) and a raking width of 2.4 m. The reel radius is 0.3 m and the head angle is $\theta_{tr} = 72°$ (7.54 rad). The reel is ground driven with a speed ratio, $v_f/v_p = 0.8$. When the rake is

traveling at 8 km/h while raking a windrow of height 0.45 m, calculate the (a) direction and (b) magnitude of the resultant tooth path, (c) the average hay velocity, (d) the maximum theoretical distance travelled by the hay during raking, and (e) ratio, v_h/v_t, of the average hay velocity to the resultant tooth velocity.

Solution. (a) Angles α_1 and α_2 must be calculated to begin the analysis. Since the angles and their trigonometric functions will be used, radians will be used instead of degrees in all of the trigonometric calculations. The value of α_2 can be calculated using equation 8.49:

$$\alpha_2 = \arccos(1 - 0.45/0.3) = 2.09 \text{ rad}$$

then all variables in equation 8.48 are known except for α_1. Because the reel has five bars, $\beta = 2\pi/5 = 1.26$ rad. Then:

$$\frac{1.26 - \alpha_1 - 2.09}{\sin(\alpha_1) + \sin(2.09)} = \frac{1}{0.8}\left[\cos(7.54) + \frac{\sin(7.54}{\tan(6.81)}\right]$$

Solving the above equation by iteration gives α_1=5.45 rad. The forward speed of the rake is 8/3.6 = 2.22 m/s and the peripheral speed of the reel is v_p=2.22/0.8=2.78 m/s. Equation 8.50 can be used to calculate the reel component, v_{tr}:

$$v_{tr} = 2.78\,[\sin(5.45) + \sin(2.09)]/[5.45 + 2.09] = 1.53 \text{ m/s}$$

Next, the direction of the resultant tooth path can be calculated using equation 8.51:

$$\theta_t = \arctan[1.53\sin(7.54)/(2.22 + 1.53\cos(7.54))] = 2.97 \text{ rad or } 28.4°$$

(b) From equation 8.52, the magnitude of the resultant tooth velocity is:

$$v_t = 1.53\ \sin(7.54)/\sin(2.97) = 3.06 \text{ m/s}$$

(c) Next, from equation 8.53, the average hay velocity is:

$$v_h = 2.22/[\cos(2.97) + \sin(2.97) + \text{cotan}(6.81)] = 1.22 \text{ m/s}$$

(d) The maximum length of the hay path, from equation 8.54, is:

$$L_h = 2.4/\sin(2.97) = 5.1 \text{ m}$$

(e) Finally, the ratio of hay velocity to tooth velocity is:

$$v_h/v_t = 1.22/3.06 = 0.40$$

The maximum hay path length is over twice the swath width and the average travel speed of the hay is only 40% of the tooth velocity. The teeth impact the hay repeatedly in moving it into the windrow and thus the leaves of legumes can be lost if the hay is very dry during raking.

Power requirements for side delivery raking are small and data are sparse. ASAE Data D497 suggests the following power requirement for a side delivery rake 2.44 m in width:

$$P_{rake} = -0.186 + 0.052\ v_f \qquad (8.58)$$

where

P_{rake} = power requirement for raking (kW)
v_f = raking speed (m/s)

Power requirements for mower-conditioners or windrowers are also sparse. Limited data suggests that the power requirement for a pto-powered windrower with sicklebar cutting, a reel and a roll-type conditioner is approximately 3.2 kW/m of width (Rotz and Sprott, 1984).

8.2.5 Baling

Hay can be harvested as loose hay in stacks or as chopped hay, but baling is the most popular method of hay harvest. The two types of balers in popular use are rectangular balers (fig. 8.6) and round balers (fig. 8.7). Although the discussion in this chapter relates to baling of hay, the same machines are used for baling straw and other fibrous materials.

Rectangular Balers. Virtually all rectangular balers have the baling chamber oriented in the direction of travel of the baler. A windrow pickup unit feeds the windrow into a cross conveyor which, in turn, feeds the hay into the baling chamber. There are three types of cross conveyors. In one type, an auger conveys the hay to a set of packer fingers which sweep the hay into the bale chamber. In a second type, linear moving packer fingers travel the full width of the pickup in conveying the hay into the bale chamber. In the third type, rotating finger wheels move the hay laterally to the packer fingers. The bale chamber is fed from below rather than from the side in one available baler. Material is fed from the pickup to the bale chamber by a crank-actuated feed fork. Feeding from the bottom allows the

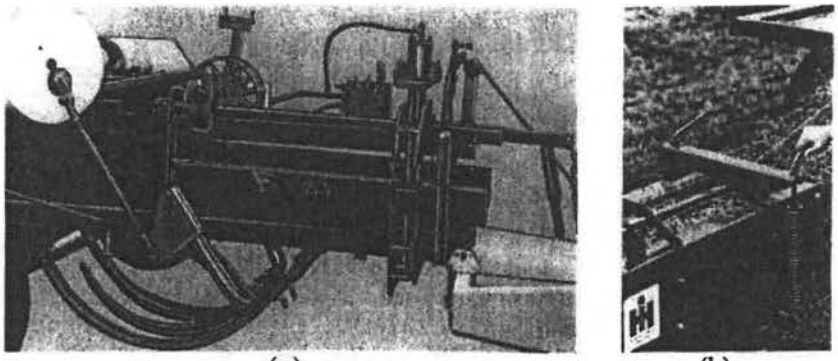

(a) (b)

Figure 8.35–Control of bale density (a) hydraulically and (b) with manually-adjustable springs (Reprinted from *Principles of Farm Machinery*, Kepner et al., 1978).

baler to travel directly behind the tractor. In all feeder designs, the packer fingers must be timed to the movement of the reciprocating plunger so that the fingers are out of the bale chamber except when the plunger is in its forward ($\theta_c = 90°$ in fig. 8.38) position.

As the feeder delivers each charge of hay, a knife on the edge of the plunger and a countershear at the rear edge of the feed opening shear off the charge of hay as the plunger moves rearward. Continued movement of the plunger compresses the charge of hay and pushes previously accumulated compressed hay through the bale chamber. Controlled convergence of the bale chamber (fig. 8.35a) provides resistance to bale movement and thus controls bale density. Fixed wedges and spring-loaded dogs extend into the bale chamber and minimize re-expansion of the compressed hay during forward movement of the plunger. During compression, a star wheel at the top of the bale chamber (the leftmost star wheel in fig. 8.35a) is driven by the moving bale to trigger the tying mechanism when a bale of sufficient length has been formed. When the plunger reaches its rearmost position after the tying mechanism has been triggered, needles (visible at bottom of fig. 8.35a) move through slots in the plunger face to deliver twine or wire to the knotter. The knotter completes the knots and the needles retract as the plunger begins moving forward.

The density of hay in the bales is determined by the type of material being baled, its moisture content, and by the resistance provided by the convergence of the bale chamber. The convergence causes the hay to be compressed laterally as the bale moves through the chamber. Assuming the hay is an elastic material, the plunger force generated by convergence can be calculated using the following equation:

$$F_c = \frac{E_h\, y}{d_c} L_c\, w_c\, f_h \qquad (8.59)$$

where

F_c = compressive force supplied by plunger (N)
E_h = effective modulus of elasticity of the hay (kPa)
L_c = length of converging section (m)
y = total convergence in converging section (mm)
d_c = depth of bale chamber (m)
w_c = width of bale chamber (m)
f_h = coefficient of friction between hay and bale chamber

The quantity, (E_h y/2 d_c) is the lateral pressure to compress the hay a distance y, and (2 L_c w_c) is the total area on which the lateral pressure acts assuming only two sides converge. Multiplying by the coefficient of friction gives the contribution of convergence to the plunger force. There will be some friction against the nonconverging sides. If all four sides converge, convergence of each pair of sides is usually controlled independently. In either case, the friction against all sides should be included in calculating F_c. Equation 8.59 is difficult to use to compute actual forces because of difficulty in determining values for E_h. However, the equation does provide insights into the problems of density control. Both E_h and f_h increase with moisture content of the hay, thus increasing the plunger force and the bale density. The tension-control springs in figure 8.35b provide the lateral force for squeezing the bales in the convergence section. Hand cranks are provided to adjust the amount of spring tension and the tension must be adjusted to compensate for changes in moisture and crop. During operation, the springs extend when E_h increases and, although y declines, the lateral force increases. Zero-rate springs would be preferable and the equivalent effect is achieved by substituting a hydraulic cylinder to provide the convergence force (fig. 8.35a). The hydraulic pressure can be adjusted from the operator's station but remains at the set value, thus providing constant force. One large rectangular baler uses several load cells placed on the plunger face to monitor the compression force. The signals from the load cells are sent to a microprocessor. The microprocessor controls bale density by sending output signals to electrohydraulic valves which control oil pressure in hydraulic cylinders which regulate bale chamber convergence. The microprocessor system ensures uniform, constant bale density as crop conditions change.

Both twine-tie and wire-tie balers are available but the twine-tie balers are much more popular. ASAE Standards S229.6 and

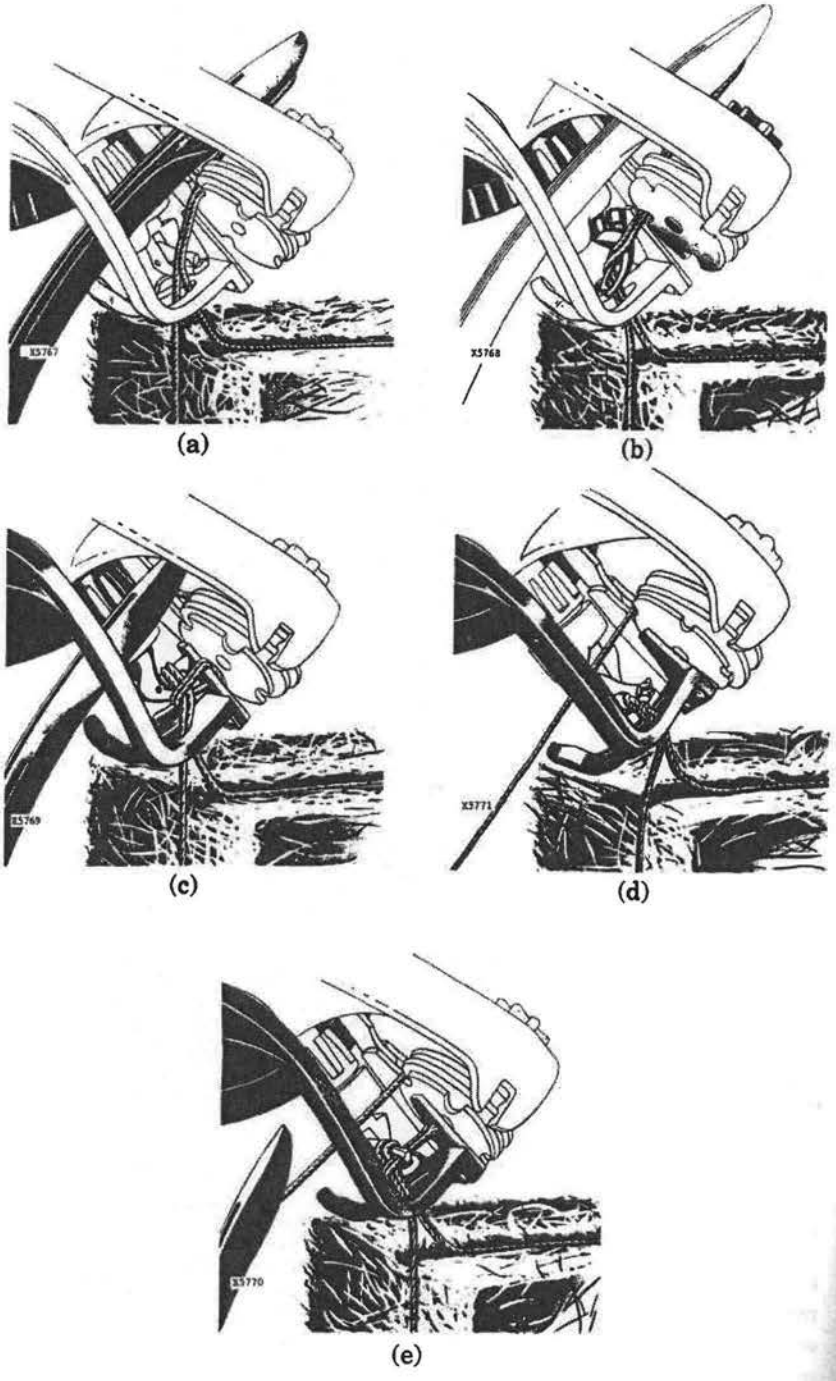

Figure 8.36–Operation of a twine knotter (Courtesy of Deere and Co.).

S315.2 provide specifications for baling wire and twine, respectively. Figure 8.36 shows a twine knotter tying a bale. In the most popular-sized baler, each bale is tied by two loops of twine and thus two knotters are included on the baler. When tying a bale, each knotter grips the cut end of its twine as the needles retract. As the next bale advances through the chamber pushing the twine strands on its leading edge, twine is pulled from two twine balls though the needle eyes. When the bale tying mechanism is triggered by the star wheel through a limited-motion pawl clutch, the needles rise through the plunger slots, carrying the twine strands to the respective knotters. Figure 8.36a shows the start of the tying cycle. The needle has brought the twine around the bale and placed it in the twine holder. The two outside disks of the holder have rotated through the angle between adjacent notches while the center disk remained stationary, thus pinching the twine between the spring-loaded disks to hold it when the needle withdraws. The knotter-bill assembly in figure 8.36b has begun rotating to form a loop in the string about the knotter bills. The loop is completed in figure 8.36c, the knotter bills have opened and, with continued rotation, the bills close over the strings held by the twine holder. As the bills grip the strings, the knife attached to the stripper arm cuts the twine between the knotter and the twine holder, thus releasing the formed bale. The bills have gripped the strings and the knife has completed the cutting in figure 8.36d and, in figure 8.36e, the wiper has completed the knot by moving forward to push the loop from the bills over the twine held by the twine holder. Note that, in figure 8.36d, the twine holder has already gripped the twine end for the next bale and continues to hold it while the current bale is being tied and the next bale is being formed. Wires are tied around bales in a manner similar to that described above, except that the wire ends are twisted, not knotted. Thus a wire-tie baler has a wire twister instead of a twine knotter. Because of the greater tensile strength of wires, wire-tied bales can have greater density than string-tied bales.

The baling rate (in kg/s) can be limited by the rate at which forage is fed into the baler, by the design of the baler or by available power. The following equation relates the first of these possible limits:

$$\dot{m}_f = \frac{d_c\, w_c\, \delta_s\, \rho_c\, n_c}{60} \tag{8.60}$$

where

$\dot{m}_f$ = baling rate or material feed rate (kg/s)
d_c = depth of bale chamber (m)
w_c = width of bale chamber (m)

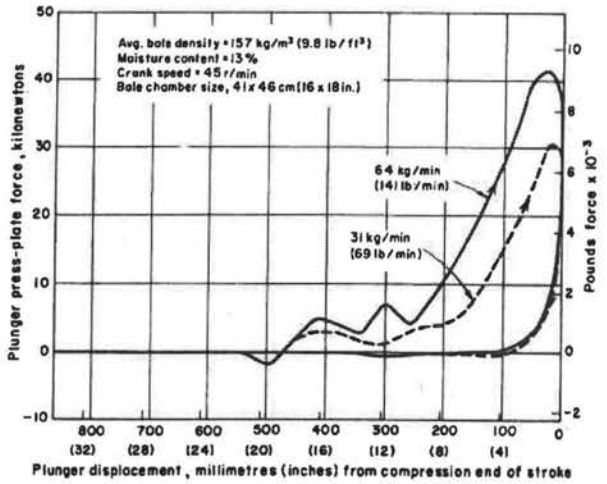

Figure 8.37–Plunger work diagrams for two feed rates in alfalfa (Burrough and Graham, 1954).

δ_s = thickness of each compressed hay slice (m)
ρ_c = compressed density of hay in bale (kg/m^3)
n_c = crank speed (rev/min)

By far the most popular chamber size is $w_c = 0.46$ m and $d_c = 0.36$ m. However, much larger balers with chambers 1.2 m by 1.2 m are on the market and several intermediate sizes are also available. Densities of hay in bales, including moisture at time of baling, range from 130 to 225 kg/m^3 with the lower end of that range being the most popular. Use of low crank speeds limits capacity and increases stress loads. Tests by Burroughs and Graham (1954) have shown that, for a given feed rate and bale density, peak plunger force fell 20% as crank speed increased from 40 to 50 rev/min but showed little decline with further increases in speed. Use of high speeds generates excessive inertia forces in the reciprocating plunger and causes greater losses of hay from the bale chamber. Practical crank speeds range from 45 rev/min for some large balers to 100 rev/min for smaller balers. Each time the baler plunger moves rearward, it shears off the incoming hay and compresses the hay charge into a flake or slice. The flake thickness varies with the rate at which hay can be fed into the bale chamber. Typically, flake thickness ranges from zero to about 20 cm. From equation 8.60, for a baler with chamber dimensions of 36 by 46 cm, crank speed of 50 rev/min, bale density of 225 kg/m^3 and flake thickness of 20 cm, the baling capacity would be 6.21 kg/s or 22.4 Mg/h. In NIAE (1965) tests of balers with the 36- by 46-cm bale chamber, rates as high as 22 Mg/h

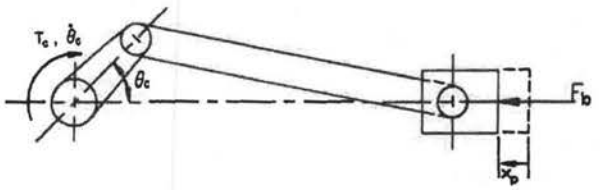

Figure 8.38–Diagram of a slider-crank mechanism in a baler.

were recorded for short time periods, but maximum rates fell to 16.3 Mg/h for continuous tests.

Instantaneous crank torque varies widely on a baler and a flywheel is used to maintain a relatively constant crank speed. Figure 8.37 shows two typical force-deflection curves for a baler plunger working with two different feed rates. The curves are similar except that compression starts earlier with the larger hay charge and the peak force is higher. The small peaks near 300 to 400 mm displacement are knife forces for shearing the hay charge; on most hay charges, these cutting peaks occur later and closer to the force peak. The force reaches a peak and begins declining when the hay compressed on earlier strokes begins moving in the chamber; the decline occurs because the sliding friction is less than the static friction in the chamber. Both force curves merge after the plunger starts forward. The force is greater than zero during the first 100 mm of return travel only because the compressed hay re-expands somewhat. During the re-expansion, a small amount of potential energy in the compressed hay is returned to the plunger in the form of kinetic energy. A force-displacement curve (fig. 8.37) can be converted to a torque versus angular displacement curve for the crank. For any given crank angle, θ_c, the plunger displacement (x_p) can be calculated using the following equation from slider-crank theory:

$$x_p = r_c (1 - \cos\theta_c) + L_{cr} - \sqrt{L_{cr}^2 - r_c^2 \sin^2\theta_c} \qquad (8.61)$$

where

x_p = plunger displacement (m) (see fig. 8.38)
r_c = crank radius (m)
L_{cr} = length of connecting rod (m)
θ_c = crank arm displacement (radians)

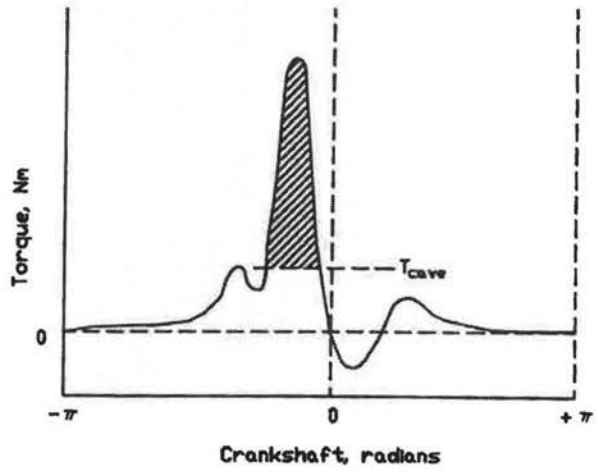

Figure 8.39–Instantaneous torque in the crank arm.

For the x_p corresponding to each θ_c, a force-displacement curve similar to the one in figure 8.37 can be used to find the corresponding plunger force. Then the instantaneous torque at that crank angle is given by the following equation:

$$T_c = \frac{-\dot{x}_p}{\dot{\theta}_c} F_p \tag{8.62}$$

where

T_c = torque in crank arm (N·m)
F_p = force on plunger (N) and

$$\frac{\dot{x}_p}{\dot{\theta}_c} = r_c \sin\theta_c + \frac{r_c \sin\theta_c \cos\theta_c}{\sqrt{\frac{L_{cr}^2}{r_c^2} - \sin^2\theta_c}} \tag{8.63}$$

where

$\dot{x}_p$ = plunger speed (m/s)
θ_c = crank speed (rad/s)

Figure 8.39 is an illustration of instantaneous crank torque. The small peak on the left is the cutting peak. The data representing instantaneous torque as a function of crank angle can be integrated numerically to obtain the average torque. The average torque, T_{cave},

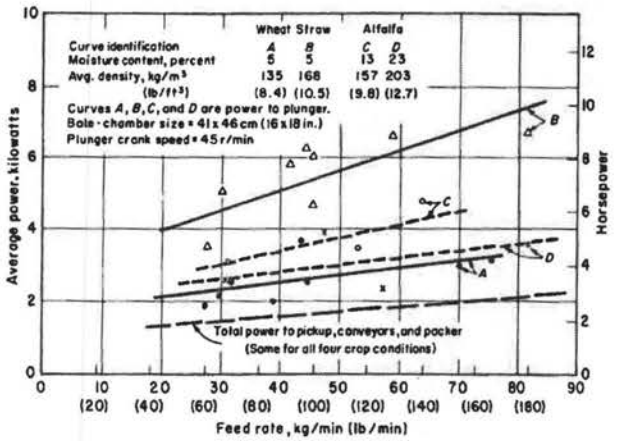

Figure 8.40–Relation of average power requirements to baling rate (Graham, 1953).

that must be supplied by the engine is shown by the dashed line across the peak. The cross-hatched area represents energy that must be supplied by a flywheel when the instantaneous torque exceeds the torque output supplied by the engine. The required flywheel size can be calculated using the following equation:

$$I_f = \frac{\Delta E_k}{R_s \dot{\theta}_{cave}^2} \tag{8.64}$$

where

I_f = mass moment of inertia of flywheel (kg·m²)
θ_{cave} = average crankshaft speed (rad/s) = (max speed – min speed)/2
ΔE_k = kinetic energy required from flywheel (J) (see fig. 8.39)
R_s = speed regulation = (max speed - min speed)/average speed

The average power required to operate the plunger can be calculated from the product of the average torque and speed at the crankshaft. It can be shown that the average torque is proportional to the area within the plunger force-displacement diagram (fig. 8.37). Note that the average torque and thus the average power requirement increase with the feed rate. The power required by the pick-up, conveyors, and packer also increase with feed rate (see fig. 8.40). The equation for the total power requirement of a baler thus has the following form:

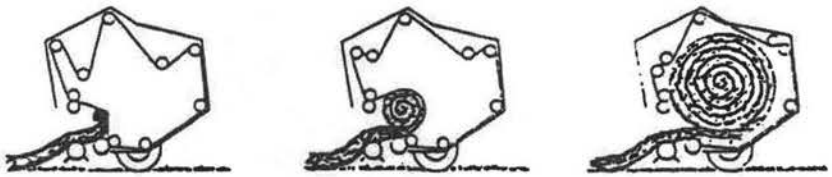

Figure 8.41-A round baler with variable geometry (Courtesy of Prairie Agricultural Machinery Institute, Canada).

$$P_{baler} = C_0 + C_1 \dot{m}_f \tag{8.65}$$

where

P_{baler} = total power requirement of baler (kW)
$\dot{m}_f$ = feed rate (kg/s)
C_0, C_1 = constants that vary with baler design, type and moisture content of material being baled. Units are kW for C_0 and kW·s/kg for C_1

Values for constants C_0 and C_1 can be determined from field tests of balers. From figure 8.40, for example, values for (C_0, C_1) are (1.75, 1.17), (2.84, 3.37), (1.88, 2.23), and (1.97, 1.23) for curves A, B, C, and D, respectively. Calculation of baler capacity and power are illustrated in example problem 8.8.

Example Problem 8.8

A rectangular baler with chamber cross-section of 0.36 m by 0.46 m is operated at a crank speed of 70 rev/min. The feed rate is such that the thickness of each compressed slice is 0.2 m and slice density is 180 kg/m^3. Power constants are C_0 = 1.88 kW and C_1 = 2.23 kW·s/kg. Calculate (a) the baler capacity, and (b) the power requirement.

Solution. (a) From equation 8.60, the capacity is:

$$\dot{m}_f = 0.36 \cdot 0.46 \cdot 0.2 \cdot 180 \cdot 70/60 = 6.95 \text{ kg/s or } 25 \text{ Mg/h}$$

(b) The baler conforms to varying feed rates by changing the slice thickness. For example, if the feed rate is increased by increasing the travel speed along the windrow, the slice thickness increases accordingly. The power requirement for the entire baler is:

$$P_{baler} = 1.88 + 2.23 \cdot 6.95 = 17.4 \text{ kW}$$

Most of the power is used in driving the plunger.

Figure 8.42–A round baler with fixed geometry (Courtesy of Prairie Agricultural Machinery Institute, Canada).

Round balers. Machines to make large round bales (fig. 8.7) entered the marketplace in 1971. ASAE Standard X498 provides terminology relating to round balers. Early machines employed a variety of techniques for forming bales, including use of variable-geometry chambers (fig. 8.41), fixed-geometry chambers, (fig. 8.42) and chambers without a floor (not shown) in which the forming bale is rolled on the ground. A pickup similar to those on rectangular balers but smaller in diameter is used to convey the windrow into the baler. When the windrow is narrower than the bale chamber, a certain amount of weaving is required by the operator to deliver hay to the full width of the chamber.

The variable-geometry chamber of figure 8.41 is the most widely used design; it creates a bale of nearly uniform density whereas the other types create bales with a low-density core. In the design of figure 8.41, a group of parallel, flat belts form the chamber. Typically, the belts are each 100 to 150 mm wide and have 50 to 100 mm wide spaces between them. The rollers on spring-loaded idler arms retract and allow the chamber to enlarge as the bale grows to full size. Power must be supplied to the chamber belts so that the moving periphery of the chamber will rotate the incoming hay and cause it to form into a tight roll. Peripheral speeds of the belts and floor conveyor typically range from 1.3 to 2.8 m/s. The chamber forms a bale with a low-density core. As additional layers are added, the density increases and is controlled by the belt tension. When the bale reaches the desired diameter, the operator stops forward motion and engages the twine-wrapping mechanism as the bale continues to rotate. A manual or powered traversing guide spaces the twine wraps at 150 to 200 mm intervals across the face of the bale. The twine is not tied; the twine end is inserted into the chamber, wraps on the bale as it rotates, is cut and left with a free end when the bale is completed. On some balers, dual-tying mechanisms allow both ends of the bale to be tied simultaneously for faster tying. As an alternative to tying with twine, the baler may be equipped with facilities for wrapping the bales in a full-width plastic netting. Only 1.5 to 2 turns of the bale are needed to wrap with netting, compared to 10 to 20 turns to wrap with twine. The netting

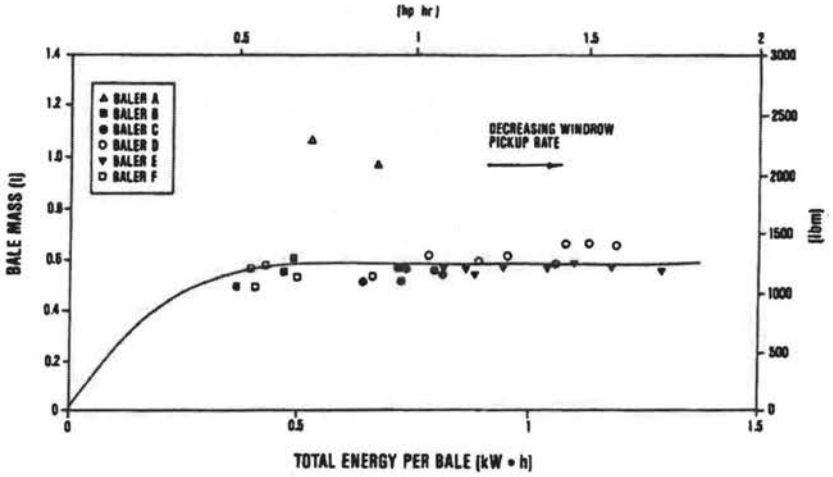

Figure 8.43–Cumulative bale mass versus energy required to form a bale (Freeland and Bledsoe, 1988).

gives the exterior of the bale a more closed structure, thus reducing leaf loss and improving weatherability compared to twine-wrapped bales. Although the netting is more expensive than twine, the improved productivity from faster wrapping, coupled with the reduced losses and improved weatherability generally offset the higher cost of the netting. After tying, the operator backs the baler approximately 6 m and raises the tailgate to eject the completed bale onto the ground. The baler is moved ahead 6 m before lowering the tail gate to allow the gate to clear the discharged bale and then baling resumes. Typical bale dimensions are 1.22 to 1.52 m in width and 1.22 to 1.83 m in diameter. Average densities range from 100 to 240 kg/m^3, giving bale masses ranging from 320 to 1050 kg per bale. Bale density varies with belt or chain tension and with belt-to-ground speed ratio. Increasing the belt speed relative to the ground speed causes thinner layers to enter the chamber and thus produces more dense bales. Good judgement must be used when ejecting bales on sloping land; ejecting bales while traveling up or down slope can allow the bales to roll downhill with great destructive potential.

Maximum instantaneous harvesting capacity of a large round baler is a product of the size of the windrow (in kg/m) and the allowable forward speed of the baler. Forward speed is typically limited by the pickup, i.e., pickup losses become excessive at very high speeds. Average travel speeds are generally in the range from 5 to 12 km/h, but average speeds up to 19 km/h have been observed. Average capacity is reduced by the time lost in tying and discharging a bale. Depending upon the windrow size, formation of a bale can take from 2 to 15 or more minutes. The tying and unloading cycle

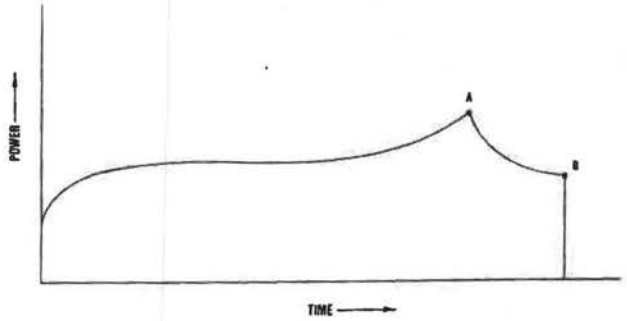

Figure 8.44–Characteristic power curve of a variable-geometry baler (Freeland and Bledsoe, 1988).

typically requires about 1 min with twine wrapping. Observed average baling rates, including the unloading cycle, have ranged from about 1 to 12 Mg/h. Since power requirements stay relatively high throughout the bale-forming process, the energy use per bale increases with the time required to form a bale (fig. 8.43). Thus, to save energy, it is advantageous to form the bales as quickly as possible.

Power requirements for operating a large round baler include pto power to form and discharge the bales, and drawbar power to propel the baler. The pto requirements follow the characteristic curve of figure 8.44, in which point A is the end of the bale-forming cycle and point B is the end of the tying cycle. The pto power requirements when the baler is running empty are typically 2 to 4 kW, but increase as the bale forms as shown in figure 8.44. With a full bale in the chamber, pto power requirements range from 12 kW to 55 kW depending on bale density and baler design. Drawbar power requirements depend heavily on field conditions as well as bale size. On firm, level fields, drawbar requirements typically range from 2.5 to 10.5 kW but the requirements can increase by 50 kW in soft, hilly fields.

8.3 Performance Evaluation

Techniques for evaluating performance can be specific to a particular machine and a wide variety of machines are used in hay and forage harvesting. For any machine, however, three types of evaluation are generally included. These are measurement of capacity, power requirements and quality of the finished product. The Prairie Agricultural Machinery Institute (PAMI) of Humboldt, Saskatchewan, Canada, conducts independent tests of various farm machines under sponsorship of several Canadian provinces. The

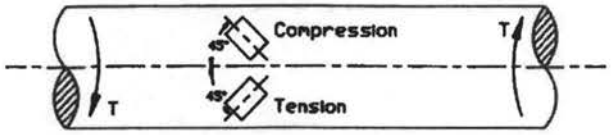

Figure 8.45–Use of strain gages to measure shaft torque.

PAMI reports are an excellent source of performance data on hay and forage harvesting equipment that is tested by PAMI.

Capacity measurements can be on the basis of area covered per unit time (in ha/h) or of material processed per unit time (in Mg/h). The amount of area that can be covered in unit time is called field capacity and is a product of the processing width and speed of the machine. Since width and speed are easily measured, field capacity measurements are not complex. For machines such as mowers, rakes, mower-conditioners, or windrowers, where the forage receives a minimum of processing, the materials handling capacity is not important and only the field capacity is measured. Conversely, the materials handling capacity is very important for forage harvesters or balers. Materials handling capacity is the maximum feed rate that can be accommodated on a sustained basis. Forage harvester feed rate is the product of mass processed per unit travel distance (for example, in kg/m) times the forward speed of the harvester. The mass per unit distance can be measured before the material enters the harvester or as it leaves. As indicated by equation 8.25, the former method involves measuring the crop yield and effective width processed by the harvester. In the latter method, the chopped material can be caught in a container for a given travel distance and then weighed. Baler feed rate can be determined by measuring the average time required to produce a bale and weighing to determine the mass in an average bale.

Power requirements of a machine include rotary power transmitted through the pto shaft and drawbar power to propel the machine. Rotary power is the product of shaft speed and shaft torque. Accurate measurement of shaft speed can be accomplished by positioning a magnetic pickup to detect passage of teeth on a gear attached to the shaft in question. Digital data loggers are available for recording the tooth passage frequency, from which the shaft speed can be determined. Measurement of torque generally involves measurement of the deflection in a given length of shaft; since shafts are designed to work within their elastic range, the deflection is proportional to the shaft torque. From strength of materials theory, shaft torque causes both tensile and compressive strains to appear on the shaft surface (see fig. 8.45). Electric resistance or semiconductor strain gages can be attached to measure these strains and thus to

measure the shaft torque. By proper positioning of the speed and torque transducers, the power demand of the various components of the machine can be measured during operation. When measuring power, it is important to simultaneously measure the other variables which affect the power requirement. Since feed rate affects the power requirement of forage harvesters and balers, the feed rate should always be measured and reported with power measurements. The moisture content of the forage should also be reported. Finally, values for all relevant machine parameters should be reported. In the case of a forage harvester, for example, the condition of the cutter knives has a large influence on the power requirement of the cutterhead. Drawbar power required to propel hay and forage machinery is usually much less than pto power and is not always reported. If drawbar power is to be reported, it can be determined by measuring travel speed and drawbar pull. Radar units are available as optional or standard equipment on many tractors and can be used to determine travel speed. As in the case of torque measurement, strain gages can be used to make a drawbar force transducer and such transducers are commercially available.

Relevant measures of quality vary with the type of machine. As examples, uniformity of stubble height may be measured for sickle bar mowers, while length of cut is important for forage harvesters. ASAE Standard S424, an ASAE standard that has been adopted by ISO as a technical report, provides methods for determining and expressing particle sizes of chopped forage. The ISO Standard DP8909-1 deals with procedures for testing forage harvesters.

Forage loss is an important parameter for all of the machines. Koegel et al. (1985) used rolled plastic to evaluate losses. Plastic sheets 3.7 m in width by 30 m in length were folded along the length to a width of 2.2 m and rolled onto spindles. A spindle was attached to a mower-conditioner and, as the plastic was unrolled during operation, the swath was deposited on the plastic. Hedge shears were used to cut and a pitchfork was used to carefully remove sections of the swath. Material remaining after the swath was removed was gathered and weighed to determine mower-conditioner loss. Next, the part of the plastic sheet that was folded underneath was pulled out and the plastic was staked at its full 3.7 m width to provide space for raking on plastic. Again, hedge shears were used to cut and a pitchfork was used to remove sections of the windrow. Material remaining after windrow removal was gathered and weighed to determine mowing plus conditioning plus raking losses. Finally, a baler was used to bale the windrows from the plastic. Additional material deposited on the plastic were attributed to baler losses. The technique did not permit separation of pickup and chamber losses from the baler. Minor damage sustained by the plastic during raking

and baling was repaired with tape. The above method used by Koegel et al. (1985) may over estimate losses. An alternative to using the plastic is to hand pick losses from the ground in small (0.25 to 0.5 m^2) sampling frames that are placed in representative areas of the field.

Length of cut is often measured when evaluating forage harvesters. Since one kilogram of chopped forage may contain over 500,000 pieces, a mechanical means of length analysis is essential (O'Dogherty, 1982). Sieving is the most common method used for length analysis, i.e., the chopped forage is passed through a series of sieves with increasingly smaller openings. A given sieve contains those lengths that passed through the sieve above but would not pass the given sieve, and the mass of that fraction is determined by weighing. The sieves must be able to size pieces which are long in relation to their cross-sectional dimensions, i.e., length to diameter ratios range up to 50:1. Sieves are oscillated to promote movement of the material; by keeping the screens horizontal and using a horizontal oscillation, the possibility of endwise movement of forage through the sieves is minimized.

Problems

8.1 A certain knife has a rake angle of 85° and a clearance angle of 2°. Calculate (a) the bevel angle and (b) the chip angle of the knife.

8.2 A rotary mower is cutting grass which leans 30° from the vertical in the direction the mower is traveling (the U-direction in fig. 8.24). Calculate the (a) tilt and (b) slant angles when $\theta = 0$, i.e., when the blade is aligned with the direction of travel. Next, calculate the (c) tilt and (d) slant angles when the blade is perpendicular to the direction of travel. Assume the forward speed of the mower is negligibly small compared to the peripheral speed of the blade.

8.3 In figure 8.8, the oblique angle of the sickle section is 30° when the forward velocity of the mower is zero, so that v_{kg} coincides with v_{km}. When the forward speed is 2.2 m/s, at what knife velocity, v_{km}, is the oblique angle zero?

8.4 In figure 8.8, the oblique angle of the sickle section is 30° when the forward speed of the mower is zero, so that v_{kg} coincides with v_{km}. (a) If the knife edge is smooth with an edge coefficient of friction of 0.306, will the plant material

slide along the edge when the knife moves toward the countershear? (b) What is the minimum coefficient of edge friction that will prevent sliding?

8.5 Assume in figure 8.8 that the leading corner of the sickle section has reached the ledger plate and the forward velocity of the mower is essentially zero. The oblique angle of the sickle section is 30°, while the oblique angle of the ledger plate is 8.4°. (a) If both the sickle section and the ledger plate have smooth edges with a coefficient of friction of 0.306, is the clip angle small enough to prevent the plant material from sliding forward along the edges? (b) Repeat part (a), except that the ledger plate is now serrated and has an edge coefficient of friction of 0.364. (c) Repeat part a, except that both the section and ledger plate have serrated edges with coefficients of friction of 0.364. (d) Suppose that forward speed of the mower has reduced the oblique angles of both the knife and the countershear by 10° and both edges have the same coefficient of friction. What is the minimum coefficient of friction that would prevent sliding?

8.6 Assume an alfalfa plant with a stem diameter of 3 mm and ultimate tensile strength of 35 N/mm^2 is being cut at a height of 60 mm above the ground, i.e., the plant roots fix the stem to the ground and the knife loads the stem as a cantilever beam. (a) How large must the knife force be to load the plant fibers to their ultimate stress? (b) If the modulus of elasticity of the stem is 1,800 N/mm^2, how far would the stem deflect when the plant fibers reached their ultimate stress?

8.7 Same as problem 8.6, except use a cotton plant with a stem diameter of 12 mm, ultimate fiber stress of 70 N/mm^2 and modulus of elasticity of 2000 N/mm^2.

8.8 Use equations 8.10 and 8.11 to generate a curve of knife force versus knife displacement during the cutting of forage. The knife width is 10 mm, the bevel angle is 20°, the clearance angle is zero, the radius of the knife edge is 0.15 mm and initial penetration occurs when the knife edge pressure on the forage reaches 20 N/mm^2. The uncompressed depth of the forage is 9 mm, the bulk modulus is 10 N/mm^2 and the coefficient of friction between forage and knife is 0.3. Assume $\lambda = 2$ in equation 8.10. Plot for knife displacements from zero to 9 mm.

8.9 Same as problem 8.8, except that the radius of the knife edge is 1.5 mm and the coefficient of friction is 0.4.

8.10 A forage harvester has eight knives on the cutterhead, which rotates at 900 rev/min. The depth of forage at initial contact of the knife is 150 mm. If the maximum cutting force is 8 kN, use equation 8.12 to estimate the power required for cutting.

8.11 Same as problem 8.10, except that the cutterhead has only four knives.

8.12 Use equation 8.16 to study the effect of stem diameter on the theoretical minimum velocity required for impact cutting. Assume that $r_g = z_{cg}$ to simplify the equation. Use equation 8.6 to calculate the bending resistance of the solid (not hollow) stem, assuming that the roots fix the stem as a cantilever beam which is struck by the knife at a distance 100 mm above the soil and the ultimate bending strength of the stem is 50 N/mm^2. Use equations 8.10 and 8.11 to estimate the knife force. Let the knife width, the uncompressed depth of material and the total knife displacement all be equal to the stem diameter; assume $\lambda = 2$, $B_f = 10$ N/mm^2, $f = 0.25$ and $\phi_{bk} = 20°$. Also, assume that the edge radius of the knife is 0.1 mm (a sharp knife) and the pressure ahead of the knife edge is 30 N/mm^2 to initiate cutting. Finally, note that the mass, m_p will vary with stem diameter, i.e., more massive plants must have larger stems to support gravitational and wind loads on the plant. Assume that $m_p = 5 \cdot 10^{-6} \cdot d^4$, where d is the stem diameter in millimeters and m_p is the plant mass in kilograms. Plot the required v_k versus stem diameter for diameters from 1 to 25 mm.

8.13 Same as problem 8.12, except use a duller knife ($r_{ek} = 1$ mm).

8.14 Same as problem 8.12, except the cut is made 2 mm above the ground.

8.15 Assuming that $\gamma = 0.3$ radians for the spatial-crank oscillator, and the input crank speed is 105 rad/s, calculate and plot values of oscillator angular displacement (Γ), velocity, and acceleration versus θ for values of θ ranging from 0 to 2π, i.e., for one full cycle.

8.16 Same as problem 8.15, except that $\gamma = 0.5$ radians.

8.17 (a) Differentiate equation 8.17b to derive an expression for the velocity of the oscillating arm. (b) Plot velocity versus input angle for one full cycle for both your derived equation and for equation 8.18 using = 0.33 radians.

8.18 (a) Derive the following equation for the knife velocity, v_{km}, assuming that knife is driven by a spatial-crank oscillator whose oscillating arm has radius r_{oa}:

$$v_{km} = (r_{oa} \cdot \omega \cdot \tan(\gamma) \cdot \cos(\theta))/(1 + \tan^2(\gamma) \cdot \sin^2(\theta))^{1.5}$$

(b) Compare the above equation to equation 8.20 in the text, which is an approximate equation for knife velocity. Note that, from the comparison:

$$r_{oa} \cdot \tan(\gamma) = \left(\frac{L_s}{2000}\right) \text{approximately}$$

(c) Further compare the two equations by plotting knife velocity versus crank angle for one full revolution of the crank. Use $\gamma = 0.3$ radians in the plots and let $L_s = 75$ mm. (d) How closely do the curves from the two equations match?

8.19 Same as problem 8.18, except $\gamma = 0.5$ radians.

8.20 Assume that the movement of the knife in figure 8.19 is governed by equation 8.20. The stroke length is 76.2 mm and the sickle frequency is constant at 105 rad/s (1000 rev/min). (Note that time, t, in equation 8.20 is measured from when the knife is in midstroke). Cutting is improved by maintaining a high knife speed through the cutting zone, i.e., from when the leading edge of the knife reaches the ledger plate until the trailing edge reaches the ledger plate. (a) Obtain an equation for knife displacement by integrating equation 8.20. Use the displacement equation to find the times when (b) the leading edge of the knife reaches the ledger plate (beginning of cutting), and (c) when the trailing edge of the knife reaches the ledger plate (end of cutting). Then, calculate the knife speed relative to the ledger plate at (d) start and (e) end of cutting. (f) Finally calculate the percent of the stroke during which cutting occurs.

8.21 Same as problem 8.20, except that the stroke length is 87 mm (i.e., the knife travels beyond the center of the ledger plate at each end of the stroke) and the sickle frequency is 84 rad/s.

8.22 Calculate the maximum inertia force on the sickle for the situation of problem 8.20 if the sickle mass is 5 kg. (Hint: differentiate equation 8.20 to obtain an equation for knife acceleration).

8.23 Calculate the maximum inertia force on the sickle for the situation of problem 8.21 if the sickle mass is 5 kg. (Hint: differentiate equation 8.20 to obtain an equation for knife acceleration).

8.24 (a) Use Elfes (1954) data that average total knife force was 1.2 kN/m of bar length when cutting frequency was 942 cycles/min in estimating the power required for cutting. Assume the standard cutting geometry as shown in figure 8.19 and let X_{bu} be equal to the effective length of stroke, i.e, the distance travelled by the knife from when the leading until the trailing edge of the knife reaches the ledger plate. (b) Using Elfes' finding that cutting used only 30% of the total pto power, estimate the total required pto power per meter of bar length. (c) Compare the answer of part b with ASAE Data 497, which suggests a pto power requirement of 1.2 kW/m for mowing alfalfa. (d) what are some of the factors that could account for differences between answers of parts b and c?

8.25 Repeat problem 8.24, except use Harbarge and Morr (1962) data that the total average knife force was 2.3 kN/m of bar length when the cutting frequency was 1250 cycles/min.

8.26 (a) A flail mower has a total of four rows of flails but, because of offsetting the flails as in figure 8.21b, there are effectively only two rows from the standpoint of stubble uniformity. Calculate and plot the ratio of stubble height difference over rotor radius (z_d/r_f) versus velocity ratio (v_f/v_p) for velocity ratios ranging from zero to 0.1. (b) On the same graph, plot a similar curve except for a six-row rotor with offset flails. If the radius of the rotor is 250 mm, what is the maximum z_d for the (c) four-row rotor and (d) six-row rotor? (d) Is a six-row rotor needed to achieve adequate stubble uniformity?

8.27 A flail mower with a rotor width of 2 m is used to mow alfalfa which has a yield of 3.2 Mg/ha. Plot the power requirement for the flail mower versus travel speed for travel speeds ranging from zero to 15 km/h.

8.28 Same as problem 8.27, except that the rotor width is 3 m.

8.29 The path of a rotary mower blade is as shown in figure 8.24. If the forward velocity, v_f, is 4% of the blade peripheral velocity, determine the maximum oblique angle and the blade angle, θ, at which it occurs. (Hint: you may find the answer either by differentiating equation 8.29 with respect to θ or by plotting oblique angle versus θ.

8.30 A rotary mower has a single blade with both ends sharpened as shown in figure 8.24. The radius of the blade is 300 mm and the blade rotates at 1900 rev/min. (a) What is the minimum width of the sharpened portion of each end of the blade, L_s, if the forward speed of the mower can be up to 4% of the peripheral speed of the blade? (b) Calculate the minimum taper of the end of the blade to prevent crop drag against the end of the blade.

8.31 Same as problem 8.30, except the blade radius is 250 mm and the blade rotates at 2200 rev/min.

8.32 (a) Estimate the power requirement of a disk-type rotary mower which has six disks, each cutting a 0.4 m width. The blades are sharp and the travel speed is 15 km/h. (b) Now estimate the power requirements for the same mower after the blades become worn.

8.33 Same as problem 8.31, except the mower is a drum-type mower.

8.34 A forage harvester has a cylindrical cutterhead 600 mm in width and 700 mm in diameter. It has eight knives and rotates at 900 rev/min. It is to harvest corn at a feed rate of 65 Mg/h while producing an average length of cut of 5 mm. The specific cutting energy can be held to 14 J·m/kg when the knives are sharp. The forage is in contact with the housing for 2.36 radians of arc and the coefficient of friction between the corn and the steel housing is 0.49. Calculate (a) the required peripheral speed of the feed rolls, (b) the maximum height of the throat area if the density between the

rolls is 300 kg/m^3, and the power requirements for (c) chopping, (d) friction, (e) impelling (assume the impeller peripheral velocity equals that of the chopper), (f) moving air, (g) the header power assuming C_{ho} = 0.6 kW and C_{R1} = 0.3 kWs/kg, and (h) the total power requirement. (i) For comparison, calculate the total power requirements using equation 8.39. (j) What length of cut would cause the answers for parts g and h to agree?

8.35 Same as problem 8.34, except only four knives are used. Also calculate the new length of cut when only four knives are used.

8.36 Same as problem 8.34, except that dull knives have allowed the specific cutting energy to rise to 28 J·m/kg.

8.37 Same as problem 8.34, except alfalfa is being harvested at a rate of 50 Mg/h, the length of cut is to be 10 mm, the density in the throat is 55 kg/m^3 and the specific cutting energy is 16 J·m/kg.

8.38 Alfalfa is cut at 80% moisture on a day when the dry bulb temperature is 30° C, the solar radiation is 700 W/m^2, and the soil moisture is 17%. The density of alfalfa in the swath is 450 g/m^2. (a) Assuming the hay is cut in a humid area, so that equation 6.41 applies, plot the moisture content of the hay versus time for 8 h of drying on the day the hay is cut. Assume no drying agent is used. (b) Add a second curve to the graph, but with 0.08 g/g of drying agent used.

8.39 Same as problem 8.38, except that the temperature is only 20° C and the solar radiation is only 350 W/m^2, i.e., it is a poorer drying day.

8.40 Same as problem 8.38, except use equation 8.45 with a vapor pressure deficit of 2.5 kPa.

8.41 Same as problem 8.38, except the swath density is reduced 20%.

8.42 A side-delivery rake with five bars in its oblique reel head has the following parameters:

raking width=02.59 m
reel radius =00.30 m

θ_{tr} =072°
γ =065°

The reel is ground driven such that $v_f / v_p = 0.82$. Assuming $y_2 = 0.2$ m, calculate and plot (a) v_h/v_f and (b) L_h/w_r for travel speeds ranging from 3 to 11 km/h.

8.43 Same as problem 8.42, except that the rake is pto driven with $v_p = 2.0$ m/s.

8.44 Same as problem 8.42, except the rake is a finger-wheel rake with the following parameters:

raking width=03.20 m
reel radius =00.74 m
θ_{tr} =0130°

8.45 (a) Estimate a value for E_h by using equation 8.59, data from figure 8.37 and assumed data as follows:

d_c = 0.46 m, from figure 8.37
w_c= 0.41 m, from figure 8.37
F_p= 42 kN, from figure 8.37
L_c= 0.70 m, assumed
y = 75 mm, assumed
f_h = 0.25, assumed

The assumed values were chosen to be realistic values for the baler used to develop figure 8.37. (b) To provide a basis for evaluating your value for E_h, Persson (1987) presented a value of 35 MPa as a limiting value beyond which straw at 20% moisture content would not compress. When the moisture content of the straw was 70%, the limiting value was 5 MPa. Since the hay compressed in the baler of figure 8.37, the value of E_h must have been less than a similar limiting value.

8.46 (a) Generalize figure 8.37 by plotting plunger compressive pressure on the y-axis versus percent of plunger stroke on the x-axis. The compressive pressure is the plunger force divided by the cross-sectional area of the plunger (bale chamber cross-section dimensions are given on fig. 8.37). Percent of stroke is the actual plunger displacement divided by the maximum displacement (547 mm in fig. 8.37). (b) Be sure to include a curve for each of the two feed rates in figure 8.37.

Generalize by using data from figure 8.37 and equation 6.60 to calculate the slice thickness, δ_s, associated with each feed rate.

8.47 (a) Calculate and plot a torque-displacement curve similar to figure 8.39 for a baler baling alfalfa hay at 13% moisture content to an average bale density of 157 kg/m^3. The chamber is 0.36 m wide by 0.46 m high, the crank radius is 0.38 m, the connecting rod length is 1.12 m and the crank speed is 79 rev/min. Note that equation 8.61 can be used to calculate the plunger displacement, for each crank angle through the full cycle. For each plunger displacement, use the plot made in problem 8.46 (with the maximum slice thickness) to determine the pressure on the plunger face and then calculate the plunger force. Then equations 8.62 and 8.63 can be used to calculate torque at each crank angle. (b) Integrate the torque-displacement curve of part a to find the average torque through the cycle. (c) Calculate the required flywheel inertia to provide 10% speed regulation, i.e., $R_s = 0.2$. (d) Calculate the power required to operate the plunger.

8.48 Same as problem 8.47, except use the minimum slice thickness from problem 8.45 b.

8.49 A large round baler is making alfalfa bales with a width of 1.5 m, diameter of 1.75 m, and average density of 200 kg/m^3. The speed of the baler while making bales is 8 km/h and the windrows contain 0.9 kg of hay per meter of length. The peripheral speed of the chamber belts is 2.75 m/s. The pto power is 3 kW when the baler is running empty, and 30 kW when a bale reaches full size. Calculate (a) the time required to form a full bale, (b) the mass of a full bale, (c) the rotational speed of the bale in the chamber when full size, (d) the torque, and (e) peripheral force that must be supplied by the belts to turn the full bale, (f) the number of rotations of the bale required to wrap twine at 150 mm spacing across the full width of the bale, and (g) the time required to wrap the twine. (h) Calculate the time savings per bale if each bale is wrapped with 1.5 turns of net wrap instead of twine.

8.50 Same as problem 8.49, except that the peripheral speed of the chamber belts is 1.5 m/s.